The genomic context and co-recruitment of SP1 affect ERRα co-activation by PGC-1α in muscle cells

Silvia Salatino[1,2,3,*,%], Barbara Kupr[1,*], Mario Baresic[1,&] , Erik van Nimwegen[2,3,#], and Christoph Handschin[1,#]

Published in Mol Endocrinol. 2016 Jul;30(7):809-25. PMID: 27182621. doi: 10.1210/me.2016-1036.

Reprint request

Unfortunately, due to copyright-relatedt issues, we are not able to post the post-print pdf version of our manuscript - in some cases, not even any version of our manuscript. Thus, if you would like to request a post-production, publisher pdf reprint, please click send an email with the request to christoph-dot-handschin_at_unibas-dot-ch (see http://www.biozentrum.unibas.ch/handschin).

Information about the Open Access policy of different publishers/journals can be found on the SHERPA/ROMEO webpage: http://www.sherpa.ac.uk/romeo/

Reprint Anfragen

Aufgrund fehlender Copyright-Rechte ist es leider nicht möglich, dieses Manuskript in der finalen Version, z.T. sogar in irgendeiner Form frei zugänglich zu machen. Anfragen für Reprints per Email an christoph-dot-handschin_at_unibas-dot-ch (s. http://www.biozentrum.unibas.ch/handschin).

Informationen zur Open Access Handhabung verschiedener Verlage/Journals sind auf der SHERPA/ROMEO Webpage verfügbar: http://www.sherpa.ac.uk/romeo/

The genomic context and co-recruitment of SP1 affect ERRα co-activation by PGC-1α in muscle cells

Silvia Salatino[1,2,3,*,%], Barbara Kupr[1,*], Mario Baresic[1,&] , Erik van Nimwegen[2,3,#], and Christoph Handschin[1,#]

[1]Focal Area Growth & Development and [2]Focal Area Computational & Systems Biology, Biozentrum, University of Basel, Basel 4056, Switzerland

[3]Swiss Institute of Bioinformatics, Basel 4056, Switzerland

Short title: Regulation of ERRα-PGC-1α coactivation

Key terms: skeletal muscle; co-activator; transcription factor; PGC-1α; ERRα; transcriptional regulation; ChIP-Seq

Word count: 9928

Number of figures and tables: 6

[#]Corresponding authors and persons to whom reprint requests should be addressed:

Christoph Handschin, Biozentrum, University of Basel, Klingelbergstrasse50/70, CH-4056 Basel, Switzerland, email: christoph.handschin@unibas.ch or Erik van Nimwegen, Biozentrum, University of Basel, Klingelbergstrasse50/70, CH-4056 Basel, Switzerland, email: erik.vannimwegen@unibas.ch

Disclosure summary: The authors have nothing to disclose.

Footnotes:

*These authors contributed equally to this manuscript

[%]Current address: Wellcome Trust Centre for Human Genetics, Roosvelt Drive, Oxford OX3 7BN, United Kingdom

[&]Current address: Schweizerische Arbeitsgemeinschaft für Klinische Krebsforschung (SAKK), Bern, Switzerland

Abstract

The peroxisome proliferator-activated receptor γ co-activator 1α (PGC-1α) coordinates the transcriptional network response to promote an improved endurance capacity in skeletal muscle, e.g. by co-activating the estrogen-related receptor α (ERRα) in the regulation of oxidative substrate metabolism. Despite a close functional relationship, the interaction between these two proteins has not been studied on a genomic level. We now mapped the genome-wide binding of ERRα to DNA in a skeletal muscle cell line with elevated PGC-1α and linked the DNA recruitment to global PGC-1α target gene regulation. We found that, surprisingly, ERRα co-activation by PGC-1α is only observed in the minority of all PGC-1α recruitment sites. Nevertheless, a majority of PGC-1α target gene expression is dependent on ERRα. Intriguingly, the interaction between these two proteins is controlled by the genomic context of response elements, in particular the relative GC and CpG content, monomeric and dimeric repeat binding site configuration for ERRα, and adjacent recruitment of the transcription factor SP1. These findings thus not only reveal a novel insight into the regulatory network underlying muscle cell plasticity, but also strongly link the genomic context of DNA response elements to control transcription factor – co-regulator interactions.

55 **Introduction**

56 Skeletal muscle cells have an enormous capacity to respond to external stimuli, e.g. altered levels of
57 physical activity, temperature, oxygen, nutrient composition and supply, by modulating metabolic and
58 contractile properties (1,2). Accordingly, skeletal muscle cell plasticity entails a biological program
59 with an enormous complexity. Thus, not surprisingly, the molecular mechanisms that control this
60 program are still largely elusive. In recent years however, the peroxisome proliferator-activated
61 receptor γ coactivator 1α (PGC-1α) has emerged as a regulatory nexus in the phenotypic adaptation of
62 skeletal muscle to endurance training (3). The expression of individual or groups of target genes is
63 positively or negatively affected by specific interactions of PGC-1α with a substantial repertoire of
64 different transcription factors (TFs) (4). The dynamism and flexibility of a coactivator-controlled
65 transcriptional network could therefore provide an explanation regarding how PGC-1α expression in
66 muscle is not only sufficient to induce a high endurance phenotype in this tissue (5,6), but also to
67 control related processes such as angiogenesis (7) or post- and pre-synaptic neuromuscular junction
68 plasticity (8).

69 The estrogen-related receptor α (ERRα, NR3B1) plays a prominent role in regulating cellular
70 metabolism that is highly reminiscent of the function of PGC-1α to boost mitochondrial biogenesis
71 and oxidative substrate utilization (9). Indeed, a close relationship between ERRα and PGC-1α in the
72 regulation of the expression of metabolic and other genes has been described in muscle and other
73 tissues (10,11). Unbiased motif prediction in promoters of genes that exhibit PGC-1α-dependent
74 changes in expression furthermore implied co-activation of ERRα by PGC-1α as a central regulatory
75 paradigm in the control of mitochondrial oxidative phosphorylation (OXPHOS) gene expression (12).
76 Intriguingly, at least in some crystal structures, the ligand-binding pocket of ERRα is almost
77 completely occupied by bulk amino acid side chains and thereby, binding of putative endogenous
78 ligands in the ligand binding pocket might be almost impossible (13). Instead, fluorescence
79 polarization-based binding assay of the ERRα ligand binding domain (LBD) together with a
80 coactivator peptide from PGC-1α revealed that these two partners exhibit a particularly high
81 interaction affinity, as well as a change of the ERRα LBD into a transcriptionally active conformation
82 in a ligand-independent manner (13). These data imply a "special relationship" between ERRα and
83 PGC-1α to constitute the mechanistic core of PGC-1α- and ERRα-controlled gene expression whereby
84 PGC-1α could act as the effective "ligand" of ERRα (14).

85 Recently, we have investigated the global DNA recruitment pattern of PGC-1α to the mouse genome
86 in muscle cells related to PGC-1α-controlled gene transcription (4). To our surprise, a computational
87 analysis of regulatory sites in positively regulated PGC-1α target genes not only suggested ERRα as an
88 important TF in the regulation of direct, but also to be involved in the induction of indirect PGC-1α
89 target genes, implying a role for ERRα in the absence of co-activation (4). To rule out the possibility

90 of false positive computational prediction or spurious assignment of different nuclear receptor binding
91 sites as ERRα response elements, we now studied genome-wide binding of endogenous ERRα to the
92 mouse genome in muscle cells upon activation of PGC-1α. As in our previous study, cultured muscle
93 cells were chosen based on their low expression of endogenous PGC-1α and hence a high signal-to-
94 noise ratio upon adenoviral overexpression of this coactivator. Furthermore, exogenous expression of
95 PGC-1α allowed the introduction of an epitope tag, which not only further enhances the selectivity of
96 the immunoprecipitation, but also circumvents the problem of the currently existing low affinity
97 antibodies that hamper an analysis of endogenous, untagged PGC-1α in cells or muscle tissue in vivo.
98 Thus, by comparing genomic loci bound by endogenous ERRα in muscle cells that overexpress PGC-
99 1α with those occupied by PGC-1α using chromatin immuno-precipitation followed by deep
100 sequencing (ChIP-Seq), we aimed at identifying shared and individual recruitment sites for these two
101 proteins in the context of PGC-1α-controlled muscle gene expression in the same cellular context. We
102 now experimentally confirmed a role for ERRα in the regulation of PGC-1α-mediated transcription,
103 thus after overexpression of PGC-1α, in the absence of PGC-1α co-recruitment. Importantly, we
104 identified several parameters describing the genomic context of DNA response elements that
105 differentiate between ERRα/PGC-1α coactivation and exclusive ERRα DNA binding. In particular,
106 monomeric/dimeric DNA binding site configuration for ERRα, GC and CpG content of the binding
107 region and co-recruitment of the specificity protein 1 (SP1) predict the interaction between PGC-1α
108 and ERRα. Collectively, these findings not only significantly expand our insights into the regulation of
109 the PGC-1α-controlled transcriptional network involved in muscle cell plasticity, but at the same time
110 provide distinctive molecular links between genomic elements and TF – coregulator interactions.

111

Materials and Methods

Cell culture, shRNA knockdown of ERRα and RNA isolation

C2C12 cell culture, shRNA-mediated knockdown and RNA isolation were performed as described (4). The adenoviral vectors for the modulation of ERRα were a generous gift from Prof. A. Kralli from the Scripps Research Institute in La Jolla, California, USA. For the ERRα knockdown gene expression arrays, the RNAs from the following three conditions were used: AV-shGFP + AV-GFP + vehicle (0.02% DMSO); AV-shGFP + AV-flag-PGC-1α + vehicle (0.02% DMSO); AV-shERRα + AV-flag-PGC-1α + 2μM XCT-790. Briefly, myoblasts were differentiated into myotubes for 4 days, infected with adenoviral constructs and treated with XCT-790 for 2 additional days with daily medium change before harvesting. XCT-790 was used in the experiment to inhibit residual ERRα activity since the AV-shERRα knockdown alone was incomplete (at approx. 20% control levels, data not shown). Since modulation of PGC-1α and ERRα could potentially affect the myogenic program, the degree of differentiation of the cells was visually assessed before each experiment. Affymetrix Mouse Genome 430 2.0 arrays were used for the gene expression analysis.

ChIP and ChIP-Seq

The ERRα ChIPseq was done in cells overexpressing PGC-1α using the exact same conditions and methodology as described for the PGC-1α ChIPseq experiments (4) and the ChIP-Seq data for PGC-1α was used from previous work (4) to assess DNA binding of ERRα in the context of PGC-1α-regulated gene expression. For the immunoprecipitation of ERRα, magnetic beads (Dynabeads Protein G, Invitrogen) were coated with the monoclonal anti-ERRα antibody (ERRα Rabbit Monoclonal Antibody, Clone ID: EPR46Y, Epitomics). For the ChIP of SP1, the magnetic beads were coated with the polyclonal anti-SP1 antibody (ChIPAb+Sp1 Rabbit Polyclonal Antibody, #17-601, Millipore).

High-throughput sequencing, read mapping and peak calling

The ERRα ChIP-Seq experiment in C2C12 cells undergoing PGC-1α over-expression was performed at the joint Quantitative Genomics core facility of the University of Basel and the Department of Biosystems Science and Engineering (D-BSSE) of the ETH Zurich in Basel on a Illumina HiSeq2000 sequencer as described (4).

The sequenced reads underwent a quality filter which retained all reads having Phred score >= 20, read length >= 25 bps and ambiguous nucleotides (Ns) per read <= 2. The reads that passed the filter were used as input for Bowtie version 0.12.7 (15) and aligned to the UCSC mm9 mouse genome assembly. Moreover, to avoid PCR amplification error, which might have arisen during sample preparation, we removed redundant reads mapping to the same location with the same orientation and we kept at most one read per position. Consequently, we obtained 2’155’507 covered positions for the

145 IP and 84'175'472 covered positions for the WCE. Peak calling was performed as described using
146 sliding windows (4). For the ERRα ChIP-Seq experiment, all consecutive windows having a Z-score
147 greater than 3.5 were merged and the top scoring one from each window cluster was considered as the
148 peak summit and used for further analyses.

149 **TF binding site over-representation and principal component analysis**

150 Analysis of TF binding site over-representation and principal component analysis was done as
151 described (4). Briefly, TF binding site occurrence was compared to a randomized background set of
152 regions and overrepresentations of TF binding sites calculated based on occurrence in peaks vs. that in
153 the shuffled, randomized background. The principal component analysis (PCA) was based on an input
154 matrix N containing the total number of predicted TF binding sites in each of the peaks for the 190
155 mammalian regulatory motifs that were defined.

156 **Gene expression array analysis and gene ontology**

157 Microarray probes were associated to a comprehensive collection of mouse promoters that was
158 downloaded from the SwissRegulon database (16) as described (4). For each promoter, the log2 fold
159 change (log2FC) was compared between the following conditions: over-expressed PGC-1α (treatment)
160 and GFP (control); ERRα knockdown with the addition of XCT-790 (treatment) and over-expressed
161 PGC-1α (control). The significance of the expression change was assessed by a Z score, which was
162 computed as:

$$Z = \frac{\bar{E}_{treatment} - \bar{E}_{control}}{\sqrt{\frac{\sigma^2{}_{treatment}}{n} + \frac{\sigma^2{}_{control}}{n}}}$$

163 where $n = 3$ was the number of replicate samples, $\bar{E}_{treatment}$ is the mean log2 expression across the
164 treatment samples, $\bar{E}_{control}$ is the mean log2 expression across the control samples, and $\sigma^2{}_{treatment}$
165 and $\sigma^2{}_{control}$ are the variances of log2 expression levels across the replicates for the treatment and
166 control samples, respectively. A log2FC threshold of ±0.585 (corresponding, in a more commonly
167 used notation, to 1.5 fold change) and a Z score cutoff of ±3 were used to identify significantly up-
168 /down-regulated promoters. The criterion used to associate peaks and genes was proximity. For each
169 gene with one or more differentially regulated promoters, we checked whether there was a peak
170 located within 10 kb from any of the gene's associated promoters. Gene ontology analysis was
171 performed as described using a false discovery rate (FDR)-adjusted p-value <= 0.05 for enrichment.

172 **Motif activity response analysis**

173 An extended version of Motif Activity Response Analysis (ISMARA, (17)) to separately model the
174 direct and indirect regulatory effects that ERRα and PGC-1α was performed as described (4) using the

following linear model with e_{ps} denoting the log-expression of promoter p, i.e. the total log-expression of transcripts expressed from that promoter, and N_{pm} denoting the total number of predicted TFBSs for regulatory motif m in the proximal promoter p (running from -500 to +500 relative to the transcription start site, or TSS):

$$e_{ps} = c_p + \tilde{c}_s + \sum_m N_{pm} A_{ms}$$

In this model, c_p describes the basal expression of promoter p, $\tilde{c}_s$ a sample-dependent normalization constant, and A_{ms} is the regulatory activity of motif m in sample s, which is inferred by the model. To extend this model to now incorporate PGC-1α and ERRα binding data, we recognized that the motif activities A_{ms} of a given regulatory motif m may be modulated by the nearby binding of PGC-1α and/or ERRα. We thus distinguished the effect A_{ms} of a regulatory site for motif m that occurs *outside* of the binding of PGC-1α/ ERRα from the effect A^*_{ms} of the motif when it occurs *within* a binding peak of either PGC-1α or ERRα. To model our gene expression data, we applied the standard MARA model above to promoters that lacked an associated PGC-1α binding peak. The gene expression changes observed at these promoters upon knockdown of ERRα and/or over-expression of PGC-1α indicate indirect regulatory effects of ERRα, PGC-1α or both of them on the activities A_{ms}. In contrast, for each "direct target" promoter p that has an associated binding peak (which could be an ERRα, a PGC-1α or an overlapping ERRα/PGC-1α peak) within 10 kb, we modelled its expression in terms of the predicted TFBSs in the binding peak, i.e.:

$$e_{ps} = c_p + \tilde{c}_s + \sum_m N^*_{pm} A^*_{ms}$$

where N^*_{pm} is the number of predicted TFBSs for motif m in the peak associated with promoter p, and A^*_{ms} is the motif activity of regulator m in sample s when this motif occurs in the context of either ERRα binding, PGC-1α recruitment or both. Besides motif activities ISMARA also calculates error-bars δ_{ms} for each motif m in each sample s. Using these, ISMARA calculates, for each motif m, an overall significance measure for the variation in motif activities across the samples analogous to a z-statistic:

$$z_m = \sqrt{\frac{1}{S}\sum_{s=1}^{S}\left(\frac{A_{ms}}{\delta_{ms}}\right)^2}$$

For each motif we calculate a z-score Z_m associated with its indirect activity changes, a z-score $Z^*_{m,ERR\alpha}$ associated with its direct activity changes in the context of ERRα binding, a z-score $Z^*_{m,PGC1\alpha}$ associated with its direct activity changes in the context of PGC-1α recruitment and a z-score $Z^*_{m,BOTH}$

201 associated with its direct activity changes in the context of both ERRα binding and PGC-1α
202 recruitment.

203 **Quantitative real-time PCR and statistical analysis**

204 Semi-quantitative real-time PCR (qPCR) was used to validate the efficiency of the ERRα knockdown
205 in regard to gene expression and to verify that the ChIP of ERRα and the ChIP of SP1 were successful.
206 The sequences of all primers used for qPCR are listed in Suppl. Table 1. Previously described ERRα
207 response elements in PGC-1α target gene promoters and known ERRα/PGC-1α target genes were used
208 as positive controls for the validation of the ChIP and gene expression, respectively. Regarding the
209 statistical analysis of qPCR data sets, the values are presented as the mean ±SEM. Student's t-tests
210 were performed and a p-value < 0.05 was considered as significant. *<0.05, **<0.01, ***<0.001.

211 **Animal experiments**

212 Mice were housed in a conventional facility with a 12-h night/12-h day cycle with free access to chow
213 diet pellet and water. For the experiments, male, 10- to 13-week-old skeletal muscle-specific PGC-1α
214 knockout (MKO) mice (18) and PGC-1α muscle-specific transgenic (Tg) animals (5) were used. All
215 experiments were performed according to the criteria outlined for the care and use of laboratory
216 animals and with approval of the veterinary office of the Basel canton and the Swiss authorities.
217 Injections were performed under sevoflurane (Provet, QN01AB08) anesthesia. Mice were injected
218 intramuscularly (i.m.) with either PBS + DMSO vehicle (30µl/TA) or Mithramycin A (Cayman
219 Chemical, 11434) (1µg/TA) dissolved in DMSO in both TA muscles. Mice were sacrificed 6 hours
220 post-injection and the TAs isolated for further analysis.

221

222 **Results**

223 ***ERRα is recruited to DNA together with and independently of PGC-1α***

224 Following up on several previous publications that implied a strong, direct co-dependence of ERRα
225 and PGC-1α in the control of PGC-1α-regulated metabolic gene expression (10,12), we previously
226 performed an unbiased, genome-wide analysis of PGC-1α recruitment to the mouse genome (4). The
227 results of this study suggested a role for ERRα in controlling PGC-1α target gene expression in the
228 absence of co-activation by PGC-1α (4). To verify these predictions and to identify all regions that are
229 bound by this TF genome-wide in skeletal muscle cells after overexpression of PGC-1α, we performed
230 a chromatin immunoprecipitation (ChIP) experiment followed by high-throughput sequencing (ChIP-
231 Seq) of endogenous ERRα in differentiated C2C12 murine myotubes that overexpressed epitope-
232 tagged PGC-1α. Thus, importantly, our experiments were not designed to map ERRα recruitment *per*
233 *se*, but specifically the involvement of ERRα in the regulation of PGC-1α muscle target genes in the
234 exact same cellular context as the previous mapping of PGC-1α recruitment (4). We then compared
235 the identified ERRα binding sites with this set of PGC-1α recruitment regions that we identified
236 previously (4). In order to identify all genomic locations significantly enriched in ERRα binding, we
237 passed a sliding window along the genome and compared the local IP read density with the
238 background read density from whole cell extract (WCE) for each consecutive window and quantified
239 the significance of the enrichment by Z score. All regions with a Z score bigger than 3.5 were merged
240 into a final total of 3225 peaks, which included binding regions in the vicinity of known ERRα target
241 genes (Suppl. Fig. S1A), like the isocitrate dehydrogenase 3 [NAD+] alpha (Idh3a) and the pyruvate
242 dehydrogenase lipoamide kinase isozyme 4 (Pdk4) (19). The enrichment of IP fragments from the
243 ChIP-Seq experiment was validated for some of these ERRα target genes by quantitative real-time
244 PCR (Suppl. Fig. S1B).

245 When we compared the genome-wide ERRα binding and PGC-1α DNA recruitment (Fig. 1A), we
246 noticed that the majority of ERRα peaks (~60%) are not overlapping a PGC-1α peak, suggesting that
247 the so-far believed concept of symbiotic cooperation between these two proteins is in fact restricted to
248 only a subset of their identified targets (~40% for ERRα and ~18% for PGC-1α), at least at the specific
249 time point of analysis chosen in our experiments. It obviously is possible that the overlap between the
250 two sets of peaks differs in a temporal manner. Moreover, the number of the PGC-1α peaks that
251 overlap ERRα binding sites (~18%) could in part be due to the high overexpression of PGC-1α.
252 Finally, the two ChIPseq experiments most likely differ in terms of specificity and efficacy of the
253 antibody-antigen interaction and thus, interpretation of negative data could be hampered in the
254 analysis. Nevertheless, the small overlap between the ERRα and PGC-1α peaks was not necessarily
255 expected based on the literature. Some examples of the differential regulation are depicted in Fig. 1B.
256 Of the 1321 ERRα peaks overlapping a PGC-1α site (that is, sharing at least one base pair), the vast
257 majority of them is well centered on the closest PGC-1α peak at a distance of a couple of dozen base

258 pairs (Fig. 1C), which could be interpreted as direct co-activation of ERRα by PGC-1α in most cases
259 of ERRα/PGC-1α peak overlap. Notably, a larger fraction of ERRα peaks (approx. 12%) resides
260 within 100 bp from a mouse promoter region (Fig. 1D), compared to the PGC-1α peaks (approx. 2%),
261 which we previously found to be more distally located (4).

262

263 ***ERRα function is required for the regulation of many PGC-1α target genes***

264 Based on DNA binding data alone, we cannot estimate how many of the non-PGC-1α overlapping
265 ERRα peaks are non-functional. Therefore, to integrate the results obtained from the ChIP-Seq
266 experiment with functional data in terms of PGC-1α-dependent gene expression, we further analyzed
267 the impact of ERRα on gene expression changes downstream of PGC-1α in differentiated muscle cells
268 using the following conditions: (i) shGFP-transfected control cells expressing small hairpin RNA
269 (shRNA) targeted at green fluorescent protein (GFP); (ii) shGFP-transfected cells expressing PGC-1α;
270 (iii) shERRα-transfected cells expressing PGC-1α in addition to shRNA against ERRα combined with
271 the ERRα inverse agonist XCT-790 (12) to completely abolish ERRα activity. By comparing
272 conditions (i) and (ii), we are able to identify gene expression changes downstream of PGC-1α
273 induction, while comparing conditions (ii) with (iii) allows us to quantify the impact of ERRα on
274 PGC-1α-mediated gene expression: for example, we observed a strong reduction of PGC-1α-
275 controlled induction of *Acadm*, a known ERRα/PGC-1α target gene, in cells with abolished ERRα
276 activity (Fig. 2A). After mapping the microarray probes to known transcripts and, through these, to a
277 reference set of mouse promoters (16), we noticed that more promoters were significantly up-regulated
278 (1863, corresponding to 1164 genes) than down-regulated (658, corresponding to 468 genes)
279 following PGC-1α overexpression; in contrast, we observed the opposite effect in the ERRα
280 knockdown cells: 910 promoters (corresponding to 597 genes) were significantly induced whereas
281 1952 promoters (corresponding to 1203 genes) were repressed, demonstrating a strong role for ERRα
282 in PGC-1α-mediated up-regulation of gene expression (Fig. 2B). Then, a region of +/- 10kb distance
283 from each promoter was chosen to assign peaks to promoters and hence divide target genes into direct
284 (harboring at least on peak within this region) vs. indirect (without a peak within this region) genes,
285 which obviously underestimates more long-range regulatory interactions. This stratification of the
286 positively regulated PGC-1α target genes in terms of presence and absence of PGC-1α and ERRα
287 peaks revealed several interesting findings: first, of the up-regulated PGC-1α target genes with a PGC-
288 1α peak within 10 kb from any of their associated promoters, which constitute roughly 40% of all up-
289 regulated PGC-1α targets, the number of genes with an overlap of ERRα and PGC-1α peaks (179
290 peaks, 15.4% of all up-regulated target genes) is lower than that of genes with only a PGC-1α peak
291 (198 genes with only a PGC-1α peak and 57 genes that harbor distinct ERRα and PGC-1α peaks, thus
292 combined representing 255 or 22% of all up-regulated genes) (Fig. 2C). Importantly, ERRα
293 recruitment is observed in a significant number of indirectly up-regulated PGC-1α target genes (166

294 genes, corresponding to 22.7% of all indirect PGC-1α targets). These data suggest that, based on DNA
295 binding, ERRα indeed plays a substantial role in PGC-1α target gene regulation, both when co-
296 activated by PGC-1α, but equally significant when binding in the absence of this co-activator.
297 Notably, the PGC-1α-mediated down-regulation of gene expression is almost exclusively indirect (439
298 out of 468 down-regulated PGC-1α target genes, corresponding to 93.8%), and the DNA binding of
299 ERRα seems to likewise play a minor role in this process with ERRα peaks occurring in only 17 of
300 down-regulated genes (3.6%) (Suppl. Fig. S2A). Of note, 62% of the 1321 overlapping PGC-1α/ERRα
301 peaks (Fig. 1A) where not associated to any gene within a distance of +/-10 kb of the TSS while 25%
302 of these peaks were linked to non-changing genes.

303 DNA recruitment of TFs or co-regulators typically only partially correlates with transcriptional
304 changes, e.g. as indicated by a large number of PGC-1α peaks that were not assigned to regulated
305 genes (4). Inversely, gene regulation can be brought about in an indirect manner and, therefore, might
306 not require a peak adjacent to the gene promoter region, as seen for 48.5% of up-regulated PGC-1α
307 target genes without a PGC-1α or ERRα peak, respectively (Fig. 2C). We classified genes that exhibit
308 up-regulation in response to PGC-1α induction into four categories based on whether they were
309 associated with a PGC-1α binding peak, i.e. direct versus indirect PGC-1α targets, and whether the up-
310 regulation was dependent on ERRα. According to this classification, approximately two thirds of the
311 up-regulated PGC-1α-controlled genes were dependent on the presence of functional ERRα protein,
312 irrespective of whether they were direct or indirect targets of PGC-1α (Figs 2D and 2E).

313 We next investigated whether the different classes of PGC-1α targets were over-represented for genes
314 from different functional categories. As expected, most of the enriched categories for ERRα-dependent
315 up-regulated target genes were related to mitochondria and oxidative energy metabolism (Fig. 2F and
316 2G). Notably, as we observed previously (4), the same functional categories show enrichment
317 regardless of direct or indirect PGC-1α involvement. Moreover, similar gene ontology terms were
318 found when using the ERRα-independent PGC-1α targets as input for FatiGO (Fig. 2F and 2G). The
319 different categories of PGC-1α target genes were confirmed by qPCR showing two ERRα-dependent
320 (*Aim1l* and *Twf2*) and two ERRα-independent (*Atg9b* and *Ifrd1*) PGC-1α target genes (Fig. 2H and 2I,
321 respectively).

322 Finally, we also checked dependency of transcriptional regulation on functional ERRα for PGC-1α
323 down-regulated targets. Peak-gene association clearly indicates that the majority of genes whose
324 transcription is repressed by PGC-1α lack peaks for either PGC-1α or ERRα within 10 kb of the gene
325 promoters (approx. 94% of all down-regulated PGC-1α target genes) (Suppl. Fig. S2A). Out of these
326 439 indirectly down-regulated genes, about 23% (101 down-regulated, indirect PGC-1α targets) were
327 dependent on ERRα meaning that PGC-1α-mediated repression was significantly alleviated by ERRα
328 knockdown (Suppl. Fig. S2B). Thus, ERRα markedly contributes to boost an indirect inhibitory
329 mechanism that is involved in PGC-1α-controlled transcriptional repression. Nevertheless, however,

330 the majority of PGC-1α-mediated inhibition of gene expression is ERRα-independent and thus using
331 alternative mediators, such as, for example, the indirect inhibition of the nuclear factor κB (NFκB)
332 (20).

333 ***Coactivation specificity of monomeric vs. dimeric ERRα binding elements***

334 In light of the postulated intimate relationship between ERRα and PGC-1α, our data depicting a high
335 degree of independence of these two proteins in the regulation of PGC-1α target genes in muscle cells
336 are quite surprising. In particular, it is unclear by what molecular mechanisms PGC-1α is recruited to
337 ERRα binding sites at some genomic loci, but not to others. ERRα can bind to a nine nucleotide-long
338 element with the consensus sequence TNAAGGTCA called an estrogen-related receptor response
339 element (ERRE) (21). In addition, binding of ERRα to repeats of ERREs and potentially other
340 response elements has also been proposed (22). In both cases, ERRα has been proposed to bind as
341 homo- or heterodimer, even to single ERREs (23). Importantly, data based on in vitro experiments
342 implied that the base at the N position of the ERRE controls co-activation by PGC-1α with a
343 preference for PGC-1α to interact with ERRα on ERREs with a T at the N position (TTAAGGTCA)
344 whereas a C (TCAAGGTCA) favors reduced co-activation by PGC-1α (22). Since these in vitro
345 studies were severely limited in terms of scope, we now investigated whether similar sequence
346 variations can be detected in a genome-wide analysis of ERRα DNA binding elements identified by
347 ChIP-Seq. We therefore split the ERRα and PGC-1α peaks into three distinct groups: "only ERRα",
348 "overlapping ERRα/PGC-1α" and "only PGC-1α" peak regions and computationally derived separate
349 binding motifs for each set of regions. Instead of inferring standard position-specific weight matrix
350 motifs, we employed a novel approach, recently developed in our group (Omidi, van Nimwegen et al.,
351 personal communication), which extends position-specific weight matrix models to so-called
352 dinucleotide weight tensors, which allow arbitrary dependencies between the positions within the
353 binding sites.

354 First, both the "only ERRα" and the "overlapping ERRα/PGC-1α" peak-associated motifs exhibited a
355 more determined 5' extension of the hexamer half-site as expected for an ERRE compared to the "only
356 PGC-1α" peak regions (Fig. 3A-C). Intriguingly, the "only ERRα" motif harbors a stronger preference
357 for C at position 5 when compared to the "overlapping ERRα/PGC-1α" peaks, even though the
358 preference for this nucleotide is relatively small. However, even more strikingly, we noticed that
359 although there are internal dependencies between the nucleotides at positions 4, 5, and 6 in every peak
360 group, the dependencies between the initial and final positions (1-2 and 13-14) of the motif are only
361 observed for "overlapping ERRα/PGC-1α" and "only PGC-1α" peaks, but not for "only ERRα" peaks
362 (Fig. 3A-C).

363 Dependencies at the ends of the motif could imply that the TF is more often binding DNA as a dimer
364 at these sites, suggesting that ERRα binding site repeats may be more likely to recruit co-activation by

365 PGC-1α than monomeric, extended half-sites. To test whether these motifs indeed differ in terms of
366 hexamer repeat configuration, we next used the core recognition motif "AGGTCA" of the ESRRA
367 weight matrix to identify nuclear receptor dimers in direct, everted or inverted configurations with a
368 variable spacing between half-sites that ranged from 1 to 10 nucleotides around the core motif in the
369 different peak groups. Remarkably, we found a striking difference in the relative occurrence of
370 monomers and dimers of nuclear receptor hexamer half-sites between the "only ERRα" and the
371 "overlapping ERRα/PGC-1α" peak sets (Fig. 3D). In the first group, the ratio of monomers to dimers
372 was markedly higher compared to the "overlapping ERRα/PGC-1α" peaks (0.63 vs. 0.32), further
373 supporting that dimeric ERRα binding sites are more likely to enable co-activation by PGC-1α.
374 Furthermore, even when the number of monomers is normalized to the sum of monomers and dimers
375 in each peak set, the "only ERRα" peaks showed the highest fraction of nuclear receptor monomers
376 (39%) of the three groups (Fig. 3D). It should be noted, however, that despite these differences, the
377 presence of a monomeric half-site in a ERRα peak is only a weak predictor of PGC-1α co-recruitment,
378 as in both groups only a marginally higher proportion of "only ERRα" peaks contain a monomer
379 compared to "overlapping ERRα/PGC-1α" ("only ERRα": 440 out of 1904 peaks corresponding to
380 23.1%; "overlapping ERRα/PGC-1α": 266 out of 1321 peaks in total corresponding to 20.1%). It is
381 therefore very likely that the sequence specificity and the monomeric/dimeric configuration favor, but
382 by themselves are not sufficient to entirely control co-activation of ERRα by PGC-1α.

383

384 ***ERRα binding regions without PGC-1α recruitment are enriched for SP1 binding***

385 To identify additional predictors of the ERRα/PGC-1α interaction, we next analyzed the occurrence of
386 TF DNA-binding motifs within all of the ERRα peaks. We used the software MotEvo to predict TF
387 binding sites (TFBSs) for a set of 190 known mammalian regulatory motifs (24). In order to explain
388 most of the binding site variation observed across the ERRα peaks, we then applied principal
389 component analysis (PCA) to a site-count matrix N, whose elements N_{pm} represent the number of
390 predicted TFBSs for each motif m in each ERRα peak region p. Out of a total of 190, the first
391 component was accounting for ~10% of the total variation in the dataset (Fig. 4A). The distribution of
392 motif projections on the first two principal components clearly indicates two distinct clusters of motifs
393 that are associated with variation along the first and second principal components (Fig. 4B). The first
394 group includes ESRRA and other nuclear receptors which have binding motifs that are very similar to
395 that of the ERRα motif. This cluster reflects the most abundant sites which can be found within the
396 ERRα binding regions. Interestingly, besides these expected nuclear receptor motifs, the second group
397 of motifs consists of GC-rich motifs which often are found in the proximity of transcriptional start
398 sites. The motif with the highest score along the first principal component describes binding elements
399 of SP1. The activity of this protein can be significantly affected by post-translational modifications,
400 resulting in SP1 to either act as an activator or as a repressor (25). Moreover, a functional link between

401 the occurrence of SP1 binding sites and ERRα activity, albeit without consideration of co-activation
402 by PGC-1α, has been proposed previously (26). We thus subsequently investigated the activity of SP1
403 in the context of PGC-1α target gene regulation. The different classes of peaks ("only ERRα", "only
404 PGC-1α", "overlapping ERRα/PGC-1α") were therefore combined with the regulation of their
405 assigned promoters ("up", "down", "non-changing", "no promoter assigned") as shown in Fig. 4C.
406 Strikingly, whenever a site for SP1 is present within a peak, it is more likely for the assigned promoter
407 to be up-regulated, strongly suggesting that in the context of PGC-1α over-expression, SP1 plays a
408 role as an activator. This effect is particularly enhanced when SP1 is found in an ERRα peak compared
409 to the PGC-1α peaks. Similarly, when analyzing TFBS predictions that differ between the "only
410 ERRα" and the "overlapping ERRα/PGC-1α" groups, SP1 emerges as the top-scoring motif and thus
411 strongly associates with "only ERRα" peaks (Fig. 4D). The specific enrichment of SP1 motifs in the
412 "only ERRα" group was also confirmed by comparing the enrichment of predicted SP1 binding sites,
413 relative to its occurrence in a set of randomized peak sequences, in "only ERRα" peaks with the
414 enrichment in "overlapping ERRα/PGC-1α" and "only PGC-1α" peaks. Although SP1 sites are more
415 frequent in all peak sets relative to randomized regions, the enrichment is by far strongest in "only
416 ERRα" peaks (Fig. 4E). Next, we experimentally validated the presence of SP1 both at the promoters
417 of the known target genes RIP140/Nrip1 and Fasn (27,28) and in ERRα peaks with an adjacent
418 predicted SP1 binding site in the proximity of four distinct genes by ChIP (Fig. 4F). Finally, we
419 studied the functional consequence of SP1 on muscle target gene expression of endogenous and
420 overexpressed PGC-1α in gain- and loss-of-function animal models *in vivo* (Suppl. Figure S3). First,
421 we validated a set of target genes belonging to all four binding categories (genes with only ERRα
422 recruitment with SP1 motifs, only ERRα recruitment without SP1 binding sites, PGC-1α/ERRα
423 overlapping peaks with SP1 motifs and PGC-1α/ERRα overlapping peaks without SP1 binding sites).
424 As shown in Fig. 5, the expression of genes from all four categories was reduced in skeletal muscle-
425 specific PGC-1α knockout (MKO) animals and elevated in skeletal muscle-specific PGC-1α
426 transgenic (mTg) mice. Thus, at least these genes are not only regulated by overexpressed PGC-1α in
427 cultured muscle cells, but also by endogenous and overexpressed PGC-1α in mouse muscle *in vivo*.
428 Subsequently, we aimed at testing the functional involvement of SP1 in the predicted subcategories of
429 PGC-1α target genes using the specific pharmacological SP1 inhibitor Mithramycin A (MitA) (29).
430 First, efficacy of SP1 inhibition was demonstrated by the reduction of the known SP1 target genes Sp1
431 and Vegfa (Suppl. Fig. S4). Surprisingly however, MitA not only reduced the ability of PGC-1α to
432 induce target genes that harbor an SP1 motif, but also those without a predicted SP1 binding site
433 (Suppl. Fig. S4). Most likely, the expected selectivity of the functional involvement of SP1 is lost due
434 to an inhibition of endogenous and transgenic PGC-1α expression by MitA (Suppl. Fig. S4). Similarly,
435 siRNA-mediated knockdown of SP1 in cultured muscle cells likewise reduced the expression of PGC-
436 1α (data not shown). Indeed, putative SP1 binding sites were found both in the proximal as well as in
437 the distal/alternative promoter regions of PGC-1α (Suppl. Fig. S4). Thus, even though we found a

438 significant functional involvement of SP1 in the regulation of PGC-1α target gene expression in mouse
439 muscle *in vivo*, we were unable to validate our prediction based on the presence of SP1 motifs in a
440 subset of these genes, most likely due to the observation of PGC-1α itself being an SP1 target.

441

442 ***ERRα peaks without PGC-1α co-recruitment exhibit higher GC and CpG content***

443 Intriguingly, the amount of predicted SP1 TFBSs (in terms of posterior sum) was much lower in PGC-
444 1α randomized (shuffled) peaks compared to the ERRα shuffled peak dataset (Fig. 4E). Since SP1 is
445 known to bind GC-rich regions, these results might reflect a different nucleotide composition between
446 the peak sets. Accordingly, we analyzed the GC and CpG content of all ERRα and PGC-1α peaks.
447 Interestingly, in contrast to the "overlapping ERRα/PGC-1α" peaks, and even more to the "only PGC-
448 1α" peaks, the "only ERRα" peaks separated into two distinct populations, one with high and the
449 second with lower GC content (Fig. 6A-C). Even more strikingly, these two populations in the "only
450 ERRα" peak group also differed in the CpG content and therefore potential CpG islands.
451 Subsequently, each peak set was further subdivided into proximal and distal binding regions, where
452 "proximal" referred to peaks within 1kb from their associated gene promoter and "distal" to peaks
453 located farther away. As clearly shown in Fig. 6D-F, the "only ERRα" peaks host more CpG
454 dinucleotides with respect to "only PGC-1α" peaks; moreover, the fraction of "only ERRα" proximal
455 peaks is much higher (~1/3) than the corresponding fraction of "only PGC-1α" peaks (~1/10).
456 Importantly, while most of this difference stems from the CpG content in proximal peaks, even the
457 more distal ERRα peak distribution curve exhibits shoulders towards higher CpG content that are
458 completely missing in the PGC-1α peaks. These results suggest a preference for high GC and CpG
459 content in ERRα DNA recruitment sites, whereas PGC-1α in the absence of ERRα is bound to
460 response elements with a relatively lower GC and CpG content. Importantly, the "overlapping
461 ERRα/PGC-1α" peaks behave in an intermediary manner (Fig. 6E).

462 Strikingly, the combination of all three parameters, monomeric binding, high CpG content and
463 presence of an SP1 binding site, synergize in discriminating between "only ERRα" and "overlapping
464 ERRα/PGC-1α" peaks. For example, as depicted in Figure 6G-H, the percentage of peaks harboring at
465 least two features are 2 fold more frequent in the "only ERRα" compared to the "overlapping
466 ERRα/PGC-1α" group, while those with all three features are even 5 times more frequent. Notably,
467 SP1 co-occurrence with high CpG content is particularly enriched in the "only ERRα" group with
468 15.7% of peaks, as opposed to only 4.5% in the "overlapping ERRα/PGC-1α" peak group. Similarly,
469 the combination of all the three criteria accounts for 6.5% of "only ERRα" peaks, whereas they are
470 found in only 1.3% of "overlapping ERRα/PGC-1α" peaks. Indeed, the CpG content, which is present
471 in 32.6% of the "only ERRα" peaks (i.e. 3 fold higher than in the other dataset), is the feature which
472 determines the biggest fraction of overlap among the three criteria that we focused on.

473 **Discussion**

474 Control of complex biological programs by co-regulator proteins has emerged as a regulatory
475 paradigm in higher organisms in recent years. For example, the three members of the steroid receptor
476 co-activator family SRC-1, -2 and -3 play a major role in modulating systems metabolism (30). Co-
477 regulator control of biological programs exhibits several advantages over individual TFs (31,32): by
478 binding to and modulating the activity of several different TFs, co-regulators usually have a broader
479 repertoire in target gene transcriptional regulation (33). Second, the possibility of coordinating the
480 regulation of genes within a specific transcriptional program provides kinetic advantages to accelerate
481 the output of specific pathways beyond the possibilities of individual gene regulation (34).
482 Furthermore, transcriptional regulation, transcript variants and a myriad of posttranslational
483 modifications allow a combinatorial control of co-regulator stability and specificity and thereby enable
484 dynamic control of complex cellular plasticity in a highly context-dependent manner (35). Many of
485 these mechanistic principles are illustrated by the regulation and function of PGC-1α in the control of
486 cellular energy homeostasis. However, mechanistic insights into the dynamic TF – co-regulator
487 interactions remain rudimentary. Following our previous report predicting ERRα activity both in the
488 presence and absence of direct PGC-1α coactivation based on motif representation (4), we now
489 provide experimental and computational evidence for a contribution of the genomic context of DNA
490 response elements to control the co-recruitment of PGC-1α and ERRα in the context of PGC-1α-
491 controlled muscle gene expression. Our findings are particularly surprising since historically, ERRα
492 has been thought to strongly rely on PGC-1α co-activation to regulate PGC-1α target gene expression
493 (10,12). Interestingly, the DNA binding of PGC-1α and ERRα have been analyzed in a previous study
494 by Charos and colleagues (36). Notably, several important differences compared to our experimental
495 system exist: for example, Charos et al. analyzed human proteins in the human hepatoma cell line
496 HepG2 and studied ERRα DNA binding in the absence of activated/elevated PGC-1α. Nevertheless, in
497 both studies, a similar number of ERRα peaks were found (3786 by Charos compared to 3225 reported
498 here), and even more importantly, the overlap between PGC-1α and ERRα peaks was likewise small:
499 of the 3193 and 1741 multiple regulatory factor binding regions (multi-RFBRs) of ERRα and PGC-1α,
500 respectively, only 535 were shared between these two factors (36).

501 Intriguingly, the decision between ERRα co-activation by PGC-1α and distinct DNA binding is to a
502 certain extent determined by several aspects of the DNA composition of the enhancer and promoter
503 regions (Fig. 6I). In particular, the ERRα binding element configuration as a monomeric half-site,
504 adjacent recruitment of SP1 and a high CpG content appear to discourage co-recruitment of PGC-1α.
505 Assuming that ERRα activity seems largely determined by coactivator action due to the small ligand-
506 binding pocket observed in some crystallographic studies (13), the context of PGC-1α-regulated gene
507 expression implies that separate ERRα DNA binding not only precludes association of PGC-1α, but
508 instead favors co-activation by other co-regulators. Indeed, the transcriptional activity of hERR1, the

509 human ortholog of the murine ERRα, is enhanced in a ligand-independent manner by the activator of
510 thyroid and retinoic acid receptors (ACTR), the glucocorticoid receptor interacting protein 1 (GRIP1),
511 and SRC-1 (37). Whether any of these co-activators are involved in ERRα-dependent muscle gene
512 regulation by PGC-1α remains to be investigated. Intriguingly, such a shift in co-activator preference
513 from PGC-1α towards binding of GRIP1 to the glucocorticoid receptor could be achieved by using
514 pharmacological means (38). Furthermore, an inverse agonist was discovered to specifically reduce
515 the interaction between PGC-1α and ERRα, but not other TF binding partners (12,39). However,
516 future studies will have to aim at determining how the genomic context translates into conformational
517 changes in a TF that then affects interaction with distinct co-regulators. Importantly, at least part of
518 this genomic context might be amenable to dynamic regulation, for example by the overall availability
519 or posttranslational control of the activity of SP1. Unfortunately, due to the potent effect of SP1 on
520 PGC-1α transcription, we were unable to validate our predictions of increased presence of SP1
521 binding sites in ERRα only regulated PGC-1α target genes. Second, the cytosines in CpG sites are
522 potential targets for DNA methylation and thereby mediate epigenetic regulation of gene expression
523 (40). Even though our conclusions rely to a large extent on computational prediction and therefore,
524 future experiments will have to further validate and expand these findings, it is intriguing to speculate
525 that DNA methylation may not only generally repress transcription by limiting TF binding, but maybe
526 in a more fine-tuned manner also modulate TF – co-regulator interactions. Moreover, based on the
527 reports of epigenetic modifications in exercise, including DNA hypomethylation of the PGC-1α
528 promoter itself (41), it thus will be interesting to study how exercise-induced epigenetic changes affect
529 not only the expression, but also the DNA recruitment and TF coactivation pattern of this key
530 regulator of endurance exercise adaptation in muscle.

531 Besides the more general implication of our results on the mechanistic aspects of genomic context, TF
532 binding and co-regulator recruitment, a second highly surprising finding emerged from the data related
533 to the function of ERRα and PGC-1α in muscle cells. Specifically, ERRα was described as the central
534 partner for PGC-1α in the regulation of mitochondrial oxidative phosphorylation gene expression
535 (10,12). Our results however now reveal a much more diverse manner by which PGC-1α regulates the
536 expression of these and other, related metabolic pathways. Ontological analysis of the PGC-1α target
537 genes devoid of an ERRα and PGC-1α peak demonstrate that other TFs also significantly contribute to
538 the regulation of genes encoding enzymes in the same metabolic pathways. Importantly, in light of the
539 close similarity of DNA binding elements and target gene activation, it is possible that some of the
540 predicted ERREs could also be activated by ERRγ. Moreover, as implied by the prediction of TF
541 binding motifs to be associated with PGC-1α-dependent transcriptional regulation, there might be a
542 number of additional TFs that work with PGC-1α in controlling muscle cell plasticity, many of which
543 have not been studied in the context of PGC-1α-mediated transcriptional control so far. Intriguingly, a
544 certain degree of functional redundancy seems to exist: for example, inhibition of ERRα reduces the
545 PGC-1α-induced expression of the vascular endothelial growth factor (VEGF) gene (7). Likewise

546 however, siRNA-mediated knockdown of components of the AP-1 TF complex or of SP1 also
547 decreases the ability of PGC-1α to increase VEGF gene expression (4). Thus, PGC-1α-controlled
548 muscle cell plasticity might combine two mechanistic principles: on the one hand, a "regulon" to
549 tightly coordinate the concurrent expression of genes that belong to a specific transcriptional program
550 while on the other hand, providing a more distributed transcriptional network using a variety of
551 different TFs, both directly as well as indirectly, to add regulatory robustness as well as flexibility to
552 control the expression of these genes in different cellular contexts. ERRα most likely is the central
553 factor for PGC-1α to control a bioenergetic regulon using several modulators including SP1 and
554 potentially others such as Prox1 (42) to affect ERRα-PGC-1α interactions. Inversely, AP-1 and other
555 TFs could complement the action of ERRα, for example by triggering muscle vascularization in
556 different contexts such as local tissue hypoxia for AP-1 as opposed to altered metabolic demand for
557 ERRα (4).

558 In conclusion, we elucidated to what extent the nuclear receptor ERRα contributes to PGC-1α target
559 gene expression in a muscle cell line. Even though our experiments were restricted to the analysis of
560 endogenous ERRα in the context of overexpressed PGC-1α in cultured muscle cells, several
561 interesting mechanistic findings emerged. Intriguingly, despite a relatively low overlap in DNA
562 binding, ERRα is crucial for the regulation of a majority of PGC-1α target genes in a muscle cell line.
563 Moreover, the genome-wide DNA binding patterns of ERRα and PGC-1α demonstrated that co-
564 activation of this TF by PGC-1α depends on different aspects of the genomic context of the DNA
565 response element. Importantly however, the postulated criteria do not provide a binary distinction
566 between co-activation and non-coactivation. Parameters with a higher predictive power might be
567 identified in a temporal analysis of PGC-1α and ERRα DNA recruitment to PGC-1α target genes in
568 muscle cells. Nevertheless, these findings not only provide important mechanistic insights into the
569 regulation of complex biological programs by co-regulator proteins, but could also help to specifically
570 modulate such networks in order to selectively address dysregulation of genes in pathological settings.
571 In the future, studies on endogenous proteins in murine and human contexts *in vivo* will help to further
572 unravel the complex mechanisms of co-activator-controlled transcriptional networks.

573

Acknowledgments

We would like to thank Dr. A. Kralli for the generous gift of control and shERRα adenoviral vectors. This project was funded by the ERC Consolidator grant 616830-MUSCLE_NET, the Swiss National Science Foundation, SystemsX.ch, the Swiss Society for Research on Muscle Diseases (SSEM), the Neuromuscular Research Association Basel (NeRAB), the Gebert-Rüf Foundation "Rare Diseases" Program, the "Novartis Stiftung für medizinisch-biologische Forschung", the University of Basel, and the Biozentrum.

Data access

The Gene Expression Omnibus (GEO) SuperSeries accession number for the ChIP-Seq and gene expression array data reported in this paper is GSE80522.

586 **References**

587 **1.** Hoppeler H, Baum O, Lurman G, Mueller M. Molecular mechanisms of muscle plasticity with
588 exercise. *Compr Physiol.* 2011;1(3):1383-1412.

589 **2.** Blaauw B, Schiaffino S, Reggiani C. Mechanisms modulating skeletal muscle phenotype.
590 *Compr Physiol.* 2013;3(4):1645-1687.

591 **3.** Pérez-Schindler J, Handschin C. New insights in the regulation of skeletal muscle PGC-1alpha
592 by exercise and metabolic diseases. *Drug Discov Today Dis Models.* 2013;10(2):e79-85.

593 **4.** Baresic M, Salatino S, Kupr B, van Nimwegen E, Handschin C. Transcriptional network analysis
594 in muscle reveals AP-1 as a partner of PGC-1alpha in the regulation of the hypoxic gene
595 program. *Mol Cell Biol.* 2014;34(16):2996-3012.

596 **5.** Lin J, Wu H, Tarr PT, Zhang CY, Wu Z, Boss O, Michael LF, Puigserver P, Isotani E, Olson EN,
597 Lowell BB, Bassel-Duby R, Spiegelman BM. Transcriptional co-activator PGC-1 alpha drives
598 the formation of slow-twitch muscle fibres. *Nature.* 2002;418(6899):797-801.

599 **6.** Handschin C, Chin S, Li P, Liu F, Maratos-Flier E, Lebrasseur NK, Yan Z, Spiegelman BM.
600 Skeletal muscle fiber-type switching, exercise intolerance, and myopathy in PGC-1alpha
601 muscle-specific knock-out animals. *J Biol Chem.* 2007;282(41):30014-30021.

602 **7.** Arany Z, Foo SY, Ma Y, Ruas JL, Bommi-Reddy A, Girnun G, Cooper M, Laznik D, Chinsomboon
603 J, Rangwala SM, Baek KH, Rosenzweig A, Spiegelman BM. HIF-independent regulation of
604 VEGF and angiogenesis by the transcriptional coactivator PGC-1alpha. *Nature.*
605 2008;451(7181):1008-1012.

606 **8.** Arnold AS, Gill J, Christe M, Ruiz R, McGuirk S, St-Pierre J, Tabares L, Handschin C.
607 Morphological and functional remodelling of the neuromuscular junction by skeletal muscle
608 PGC-1alpha. *Nat Commun.* 2014;5:3569.

609 **9.** Eichner LJ, Giguere V. Estrogen related receptors (ERRs): a new dawn in transcriptional
610 control of mitochondrial gene networks. *Mitochondrion.* 2011;11(4):544-552.

611 **10.** Schreiber SN, Emter R, Hock MB, Knutti D, Cardenas J, Podvinec M, Oakeley EJ, Kralli A. The
612 estrogen-related receptor alpha (ERRalpha) functions in PPARgamma coactivator 1alpha
613 (PGC-1alpha)-induced mitochondrial biogenesis. *Proc Natl Acad Sci U S A.*
614 2004;101(17):6472-6477.

615 **11.** Huss JM, Kopp RP, Kelly DP. Peroxisome proliferator-activated receptor coactivator-1alpha
616 (PGC-1alpha) coactivates the cardiac-enriched nuclear receptors estrogen-related receptor-
617 alpha and -gamma. Identification of novel leucine-rich interaction motif within PGC-1alpha. *J*
618 *Biol Chem.* 2002;277(43):40265-40274.

619 **12.** Mootha VK, Handschin C, Arlow D, Xie X, St Pierre J, Sihag S, Yang W, Altshuler D, Puigserver
620 P, Patterson N, Willy PJ, Schulman IG, Heyman RA, Lander ES, Spiegelman BM. Erralpha and

621 Gabpa/b specify PGC-1alpha-dependent oxidative phosphorylation gene expression that is
622 altered in diabetic muscle. *Proc Natl Acad Sci U S A.* 2004;101(17):6570-6575.

623 **13.** Kallen J, Schlaeppi JM, Bitsch F, Filipuzzi I, Schilb A, Riou V, Graham A, Strauss A, Geiser M,
624 Fournier B. Evidence for ligand-independent transcriptional activation of the human
625 estrogen-related receptor alpha (ERRalpha): crystal structure of ERRalpha ligand binding
626 domain in complex with peroxisome proliferator-activated receptor coactivator-1alpha. *J Biol*
627 *Chem.* 2004;279(47):49330-49337.

628 **14.** Handschin C, Mootha VK. Estrogen-related receptor alpha (ERRalpha): A novel target in type
629 2 diabetes. *Drug Discov Today Ther Strateg.* 2005;2(2):151-156.

630 **15.** Langmead B, Trapnell C, Pop M, Salzberg SL. Ultrafast and memory-efficient alignment of
631 short DNA sequences to the human genome. *Genome Biol.* 2009;10(3):R25.

632 **16.** Pachkov M, Balwierz PJ, Arnold P, Ozonov E, van Nimwegen E. SwissRegulon, a database of
633 genome-wide annotations of regulatory sites: recent updates. *Nucleic Acids Res.*
634 2013;41(Database issue):D214-220.

635 **17.** Balwierz PJ, Pachkov M, Arnold P, Gruber AJ, Zavolan M, van Nimwegen E. ISMARA:
636 automated modeling of genomic signals as a democracy of regulatory motifs. *Genome Res.*
637 2014;24(5):869-884.

638 **18.** Perez-Schindler J, Summermatter S, Santos G, Zorzato F, Handschin C. The transcriptional
639 coactivator PGC-1alpha is dispensable for chronic overload-induced skeletal muscle
640 hypertrophy and metabolic remodeling. *Proc Natl Acad Sci U S A.* 2013;110(50):20314-20319.

641 **19.** Zhang Y, Ma K, Sadana P, Chowdhury F, Gaillard S, Wang F, McDonnell DP, Unterman TG,
642 Elam MB, Park EA. Estrogen-related receptors stimulate pyruvate dehydrogenase kinase
643 isoform 4 gene expression. *J Biol Chem.* 2006;281(52):39897-39906.

644 **20.** Eisele PS, Salatino S, Sobek J, Hottiger MO, Handschin C. The peroxisome proliferator-
645 activated receptor gamma coactivator 1alpha/beta (PGC-1) coactivators repress the
646 transcriptional activity of NF-kappaB in skeletal muscle cells. *J Biol Chem.* 2013;288(4):2246-
647 2260.

648 **21.** Sladek R, Bader JA, Giguere V. The orphan nuclear receptor estrogen-related receptor alpha
649 is a transcriptional regulator of the human medium-chain acyl coenzyme A dehydrogenase
650 gene. *Mol Cell Biol.* 1997;17(9):5400-5409.

651 **22.** Barry JB, Laganiere J, Giguere V. A single nucleotide in an estrogen-related receptor alpha
652 site can dictate mode of binding and peroxisome proliferator-activated receptor gamma
653 coactivator 1alpha activation of target promoters. *Mol Endocrinol.* 2006;20(2):302-310.

654 **23.** Horard B, Vanacker JM. Estrogen receptor-related receptors: orphan receptors desperately
655 seeking a ligand. *J Mol Endocrinol.* 2003;31(3):349-357.

656 **24.** Arnold P, Erb I, Pachkov M, Molina N, van Nimwegen E. MotEvo: integrated Bayesian
657 probabilistic methods for inferring regulatory sites and motifs on multiple alignments of DNA
658 sequences. *Bioinformatics.* 2012;28(4):487-494.

659 **25.** Chu S. Transcriptional regulation by post-transcriptional modification--role of
660 phosphorylation in Sp1 transcriptional activity. *Gene.* 2012;508(1):1-8.

661 **26.** Castet A, Herledan A, Bonnet S, Jalaguier S, Vanacker JM, Cavailles V. Receptor-interacting
662 protein 140 differentially regulates estrogen receptor-related receptor transactivation
663 depending on target genes. *Mol Endocrinol.* 2006;20(5):1035-1047.

664 **27.** Nichol D, Christian M, Steel JH, White R, Parker MG. RIP140 expression is stimulated by
665 estrogen-related receptor alpha during adipogenesis. *J Biol Chem.* 2006;281(43):32140-
666 32147.

667 **28.** Samson SL, Wong NC. Role of Sp1 in insulin regulation of gene expression. *J Mol Endocrinol.*
668 2002;29(3):265-279.

669 **29.** Malek A, Nunez LE, Magistri M, Brambilla L, Jovic S, Carbone GM, Moris F, Catapano CV.
670 Modulation of the activity of Sp transcription factors by mithramycin analogues as a new
671 strategy for treatment of metastatic prostate cancer. *PLoS One.* 2012;7(4):e35130.

672 **30.** Stashi E, York B, O'Malley BW. Steroid receptor coactivators: servants and masters for control
673 of systems metabolism. *Trends Endocrinol Metab.* 2014;25(7):337-347.

674 **31.** Mouchiroud L, Eichner LJ, Shaw RJ, Auwerx J. Transcriptional coregulators: fine-tuning
675 metabolism. *Cell Metab.* 2014;20(1):26-40.

676 **32.** Dasgupta S, Lonard DM, O'Malley BW. Nuclear receptor coactivators: master regulators of
677 human health and disease. *Annu Rev Med.* 2014;65:279-292.

678 **33.** Handschin C, Spiegelman BM. Peroxisome proliferator-activated receptor gamma coactivator
679 1 coactivators, energy homeostasis, and metabolism. *Endocr Rev.* 2006;27(7):728-735.

680 **34.** Spiegelman BM, Heinrich R. Biological control through regulated transcriptional coactivators.
681 *Cell.* 2004;119(2):157-167.

682 **35.** Lonard DM, O'Malley B W. Nuclear receptor coregulators: judges, juries, and executioners of
683 cellular regulation. *Mol Cell.* 2007;27(5):691-700.

684 **36.** Charos AE, Reed BD, Raha D, Szekely AM, Weissman SM, Snyder M. A highly integrated and
685 complex PPARGC1A transcription factor binding network in HepG2 cells. *Genome Res.*
686 2012;22(9):1668-1679.

687 **37.** Xie W, Hong H, Yang NN, Lin RJ, Simon CM, Stallcup MR, Evans RM. Constitutive activation of
688 transcription and binding of coactivator by estrogen-related receptors 1 and 2. *Mol*
689 *Endocrinol.* 1999;13(12):2151-2162.

690 **38.** Coghlan MJ, Jacobson PB, Lane B, Nakane M, Lin CW, Elmore SW, Kym PR, Luly JR, Carter GW,
691 Turner R, Tyree CM, Hu J, Elgort M, Rosen J, Miner JN. A novel antiinflammatory maintains
692 glucocorticoid efficacy with reduced side effects. *Mol Endocrinol.* 2003;17(5):860-869.

693 **39.** Willy PJ, Murray IR, Qian J, Busch BB, Stevens WC, Jr., Martin R, Mohan R, Zhou S, Ordentlich
694 P, Wei P, Sapp DW, Horlick RA, Heyman RA, Schulman IG. Regulation of PPARgamma
695 coactivator 1alpha (PGC-1alpha) signaling by an estrogen-related receptor alpha (ERRalpha)
696 ligand. *Proc Natl Acad Sci U S A.* 2004;101(24):8912-8917.

697 **40.** Blattler A, Farnham PJ. Cross-talk between site-specific transcription factors and DNA
698 methylation states. *J Biol Chem.* 2013;288(48):34287-34294.

699 **41.** Barres R, Yan J, Egan B, Treebak JT, Rasmussen M, Fritz T, Caidahl K, Krook A, O'Gorman DJ,
700 Zierath JR. Acute exercise remodels promoter methylation in human skeletal muscle. *Cell*
701 *Metab.* 2012;15(3):405-411.

702 **42.** Charest-Marcotte A, Dufour CR, Wilson BJ, Tremblay AM, Eichner LJ, Arlow DH, Mootha VK,
703 Giguere V. The homeobox protein Prox1 is a negative modulator of ERR{alpha}/PGC-1{alpha}
704 bioenergetic functions. *Genes Dev.* 2010;24(6):537-542.

705

706

707 **Figure Legends**

708

709 **Figure 1. ERRα and PGC-1α are recruited to both shared and distinct sets of DNA elements and**
710 **target genes.** (**A**) Venn diagram depicting the number of ChIP-Seq binding peaks for PGC-1α (blue)
711 and for ERRα (cyan). (**B**) PGC-1α and ERRα read densities around the TSS of the genes Btbd1 (only
712 ERRα peak), Ldhb (overlapping ERRα/ PGC-1α peaks) and Tusc2 (only PGC-1α peak) obtained from
713 the UCSC Genome Browser. (**C**) Distribution of ERRα peaks relative to their closest PGC-1α peaks.
714 (**D**) Distribution of all ERRα peaks from the nearest mouse promoter region.

715

716 **Figure 2. PGC-1α directly up-regulates both in an ERRα-dependent and -independent manner.**
717 (**A**) qPCR analysis of PGC-1α, ERRα and Acadm mRNA levels in response to PGC-1α over-
718 expression (OV) and shERRα knockdown (KD) + XCT-790. Data are normalized to mRNA levels in
719 GFP infected cells. Error bars represent ± SEM. *p < 0.05; **p < 0.01; ***p < 0.001. (**B**) Reverse
720 cumulative distribution of log2 fold changes for all mouse promoters in the PGC-1α OV condition
721 versus GFP control (left panel) and in the PGC-1α OV + shERRα KD + XCT-790 versus PGC-1α OV
722 (right panel). Promoters are colored in red (up-regulation) when their fold change is bigger than 1.5
723 and in green (down-regulation) when their fold change is smaller than -1.5 (obtained by taking the
724 inverse of the linear binding ratio). (**C**) Tree diagram of all PGC-1α up-regulated target genes,
725 distinguished in different subgroups according to peak presence/absence. (**D**) Pie-chart representing
726 the classification of directly up-regulated PGC-1α target genes in ERRα-dependent (orange) and
727 ERRα-independent (yellow) targets. (**E**) Pie-chart representing the classification of indirectly up-
728 regulated PGC-1α target genes in ERRα-dependent (violet) and ERRα-independent (lilac) targets. (**F-**
729 **G**) Subset of the top significantly enriched GO terms identified for ERRα-dependent and ERRα-
730 independent PGC-1α directly (**F**) or indirectly (**G**) induced target genes. Abbreviations: gener.,
731 generation; metab. metabolites; * oxidoreductase activity, acting on a sulfur group, disulfide as
732 acceptor; ** S-adenosylmethionine-dependent methyltransferase activity. (**H-I**) qPCR analysis of two
733 ERRα-dependent (**H**) or ERRα-independent (**I**) PGC-1α target genes, in response to PGC-1α OV and
734 shERRα KD + XCT-790. Data are normalized to mRNA levels in GFP infected cells. Error bars
735 represent ± SEM. *p < 0.05; **p < 0.01; ***p < 0.001.

736

737 **Figure 3. In the absence of a direct coactivation by PGC-1α, ERRα prefers to bind to monomeric**
738 **DNA elements.** (**A-C**) Motif logo showing the interdependencies between the different positions of
739 the ESRRA weight matrix identified in "only ERRα", "overlapping ERRα/PGC-1α" and "only PGC-
740 1α". Dependencies between positions are indicated by a blue curved line, while yellow ellipses

741 highlight the dependencies which are in "overlapping ERRα/PGC-1α" and "only PGC-1α" peaks, but
742 not in "only ERRα" peaks. (**D**) Table showing the posterior sum and the fraction of nuclear receptor
743 hexamer half-site monomers and dimers across our three peak sets.

744

745 **Figure 4. SP1 is the top transcription factor partner for ERRα in skeletal muscle.** (**A**) Fraction of
746 explained variance of the top 10 PCA components. (**B**) PCA analysis of the 3225 ERRα peaks. The
747 names of the motifs with the largest projections on the first two principal components are indicated.
748 Purple and light blue ellipses highlight motif clusters, as identified by PC1, of nuclear hormone
749 receptor-like motifs and SP1-like motifs, respectively. (**C**) Bar chart representing the different classes
750 of peaks ("only ERRα", "only PGC1α", "overlapping ERRα and PGC1α") together with the regulation
751 of their associated promoters ("up", "down", "non-changing", "no promoter assigned"). Numbers
752 shown on top of each box represent the absolute peak counts. (**D**) Top scoring results of motif search
753 obtained by comparing the TFBSs predictions within the "only ERRα peaks" with those in the
754 "overlapping ERRα/PGC-1α". The motifs corresponding to the SP-1 group in the PCA are colored in
755 blue. (**E**) TFBSs posterior sum for SP1 in "only ERRα", "overlapping ERRα/PGC-1α" and "only
756 PGC-1α" peaks. For each dataset, TFBS occurrences were compared against binding site predictions
757 performed on the corresponding background set of shuffled peaks. (**F**) qPCR validation of the ChIP
758 enrichment measured at the promoter of a set of SP1 known target genes and around the predicted SP1
759 site within the ERRα peaks associated to the genes Pdpr, Lrpprc, Acot13 and Mul1. Bars represent
760 fold enrichment over that of the 18S rRNA gene, error bars represent SEM. *$p < 0.05$; **$p < 0.01$;
761 ***$p < 0.001$.

762

763 **Figure 5. Target genes of all four binding categories are regulated by endogenous and**
764 **overexpressed PGC-1α in mouse muscle *in vivo*.** (**A-D**) The expression of PGC-1α target genes with
765 only ERRα DNA binding with (**A**) and without (**B**) adjacent SP1 motifs as well as of PGC-1α target
766 genes with overlapping PGC-1α and ERRα peaks with (**C**) and without (**D**) SP1 binding sites was
767 validated in skeletal muscle-specific PGC-1α knockout (MKO) and transgenic (mTG) mice compared
768 to the respective wildtype littermate controls.

769

770 **Figure 6. "Only ERRα" peaks prefer to occur as ERRE monomers and to bind high CpG**
771 **content regions** (**A-C**) Two-dimensional histogram (shown as a heat map) of the GC base content
772 (horizontal axis) and CpG dinucleotide content (vertical axis) of "only PGC-1α" (**A**), "overlapping
773 ERRα/PGC-1α" (**B**) and "only ERRα" peaks (**C**). The values shown on both axes are expressed as

774 logarithms. (**D-F**) Density plots of the CpG content of "only ERRα" (**D**), "overlapping ERRα/PGC-
775 1α" (**E**) and "only PGC-1α" (**F**) peaks, located either proximally (≤ 1 kb) or distally (> 1 kb) from the
776 closest promoter. Each inset shows the bar plot of the number of "proximal" and "distal" peaks. (**G-H**)
777 Euler diagram of "only ERRα peaks" (**G**) and of "overlapping ERRα/PGC-1α" peaks (**H**). Peaks were
778 subdivided according to three different criteria: presence of SP1 binding sites, presence of monomers
779 and high CpG content (defined as GC content >= 50% and CpG content >= 65%). (**I**) Model of ERRα
780 regulation of PGC-1α target genes in muscle cells. A combination of SP1 co-recruitment, monomeric
781 vs. dimeric ERRα binding site configuration, nucleotide preference of the ERRE, and GC/CpG content
782 affect co-activation of ERRα by PGC-1α in the regulation of PGC-1α target genes in muscle cells.

783

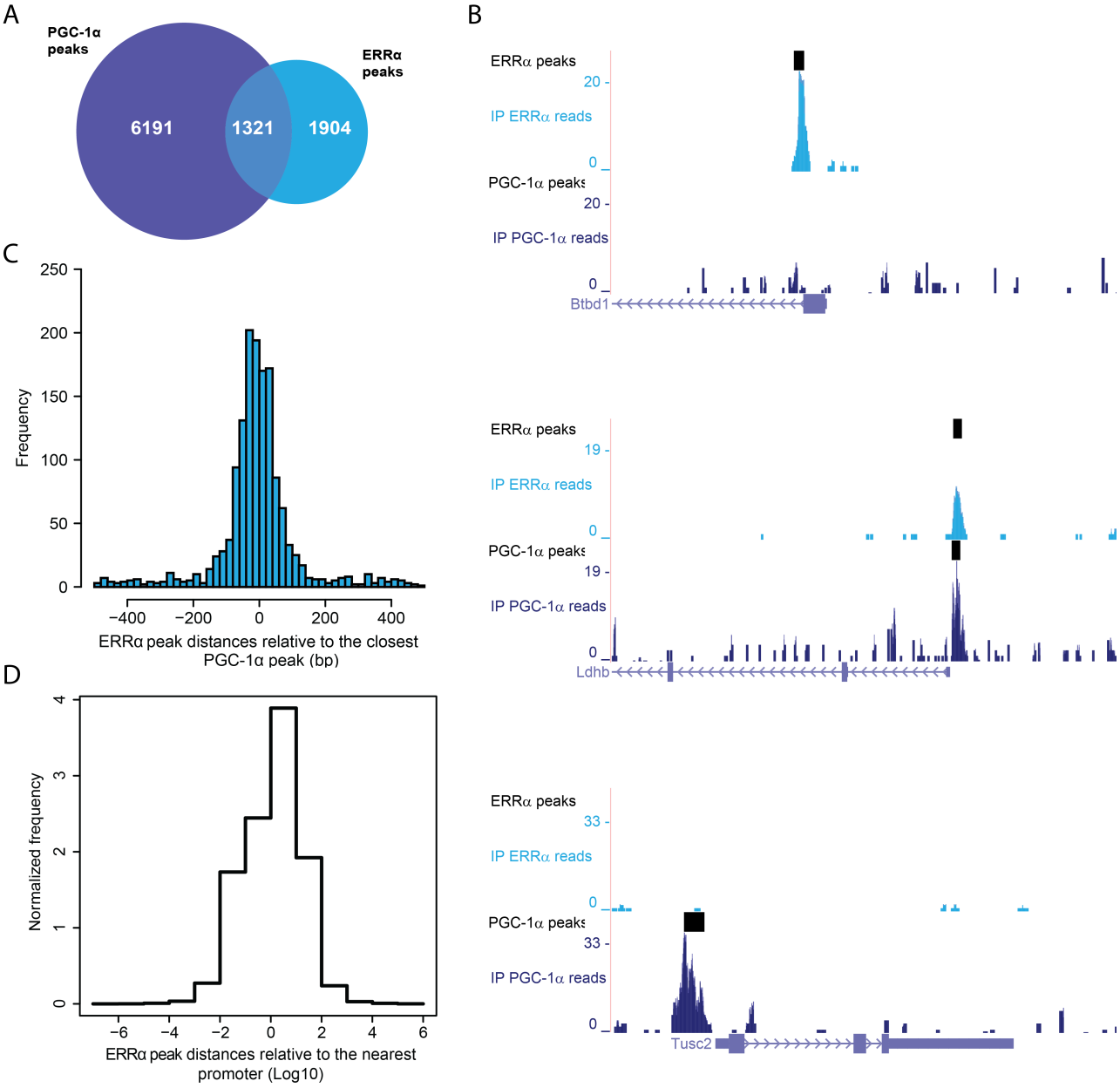
A
PGC-1α peaks
ERRα peaks
6191
1321
1904
B
ERRα peaks
20
IP ERRα reads
0
PGC-1α peaks
20
IP PGC-1α reads
0
Btbd1
ERRα peaks
19
IP ERRα reads
0
PGC-1α peaks
19
IP PGC-1α reads
0
Ldhb
ERRα peaks
33
IP ERRα reads
0
PGC-1α peaks
33
IP PGC-1α reads
0
Tusc2
C
Frequency
250
200
150
100
50
0
−400
−200
0
200
400
ERRα peak distances relative to the closest PGC-1α peak (bp)
D
Normalized frequency
4
3
2
1
0
−6
−4
−2
0
2
4
6
ERRα peak distances relative to the nearest promoter (Log10)

Figure 1

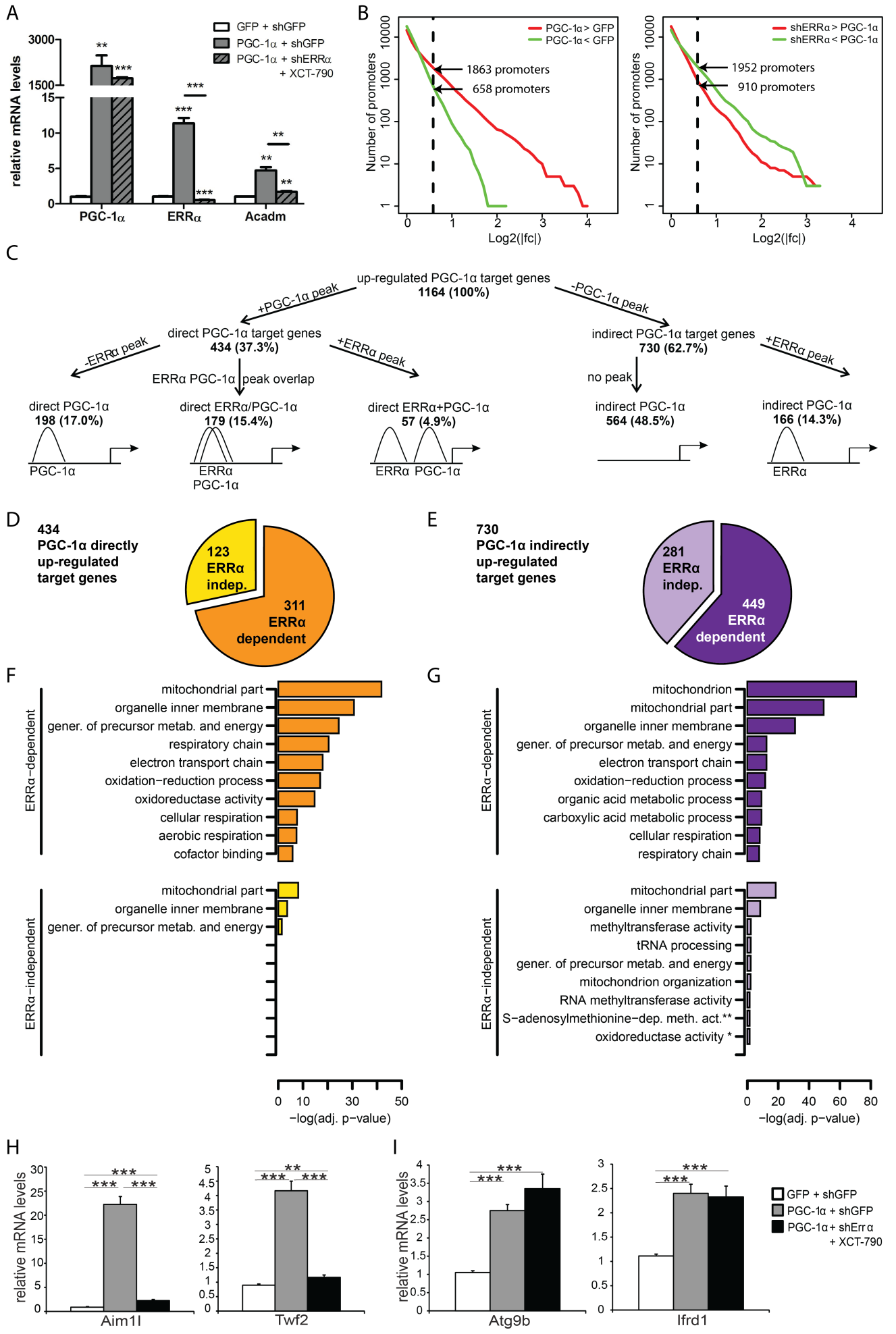
A
GFP + shGFP
PGC-1α + shGFP
PGC-1α + shERRα + XCT-790
relative mRNA levels
PGC-1α
ERRα
Acadm
B
PGC-1α > GFP
PGC-1α < GFP
1863 promoters
658 promoters
Number of promoters
Log2(|fc|)
shERRα > PGC-1α
shERRα < PGC-1α
1952 promoters
910 promoters
C
up-regulated PGC-1α target genes
1164 (100%)
+PGC-1α peak
-PGC-1α peak
direct PGC-1α target genes
434 (37.3%)
indirect PGC-1α target genes
730 (62.7%)
-ERRα peak
+ERRα peak
ERRα PGC-1α peak overlap
no peak
direct PGC-1α
198 (17.0%)
direct ERRα/PGC-1α
179 (15.4%)
direct ERRα+PGC-1α
57 (4.9%)
indirect PGC-1α
564 (48.5%)
indirect PGC-1α
166 (14.3%)
PGC-1α
ERRα
D
434
PGC-1α directly up-regulated target genes
123 ERRα indep.
311 ERRα dependent
E
730
PGC-1α indirectly up-regulated target genes
281 ERRα indep.
449 ERRα dependent
F
ERRα−dependent
mitochondrial part
organelle inner membrane
gener. of precursor metab. and energy
respiratory chain
electron transport chain
oxidation−reduction process
oxidoreductase activity
cellular respiration
aerobic respiration
cofactor binding
ERRα−independent
mitochondrial part
organelle inner membrane
gener. of precursor metab. and energy
−log(adj. p−value)
G
ERRα−dependent
mitochondrion
mitochondrial part
organelle inner membrane
gener. of precursor metab. and energy
electron transport chain
oxidation−reduction process
organic acid metabolic process
carboxylic acid metabolic process
cellular respiration
respiratory chain
ERRα−independent
mitochondrial part
organelle inner membrane
methyltransferase activity
tRNA processing
gener. of precursor metab. and energy
mitochondrion organization
RNA methyltransferase activity
S−adenosylmethionine−dep. meth. act.**
oxidoreductase activity *
−log(adj. p−value)
H
relative mRNA levels
Aim1l
Twf2
I
relative mRNA levels
Atg9b
Ifrd1
GFP + shGFP
PGC-1α + shGFP
PGC-1α + shErrα + XCT-790

Figure 2

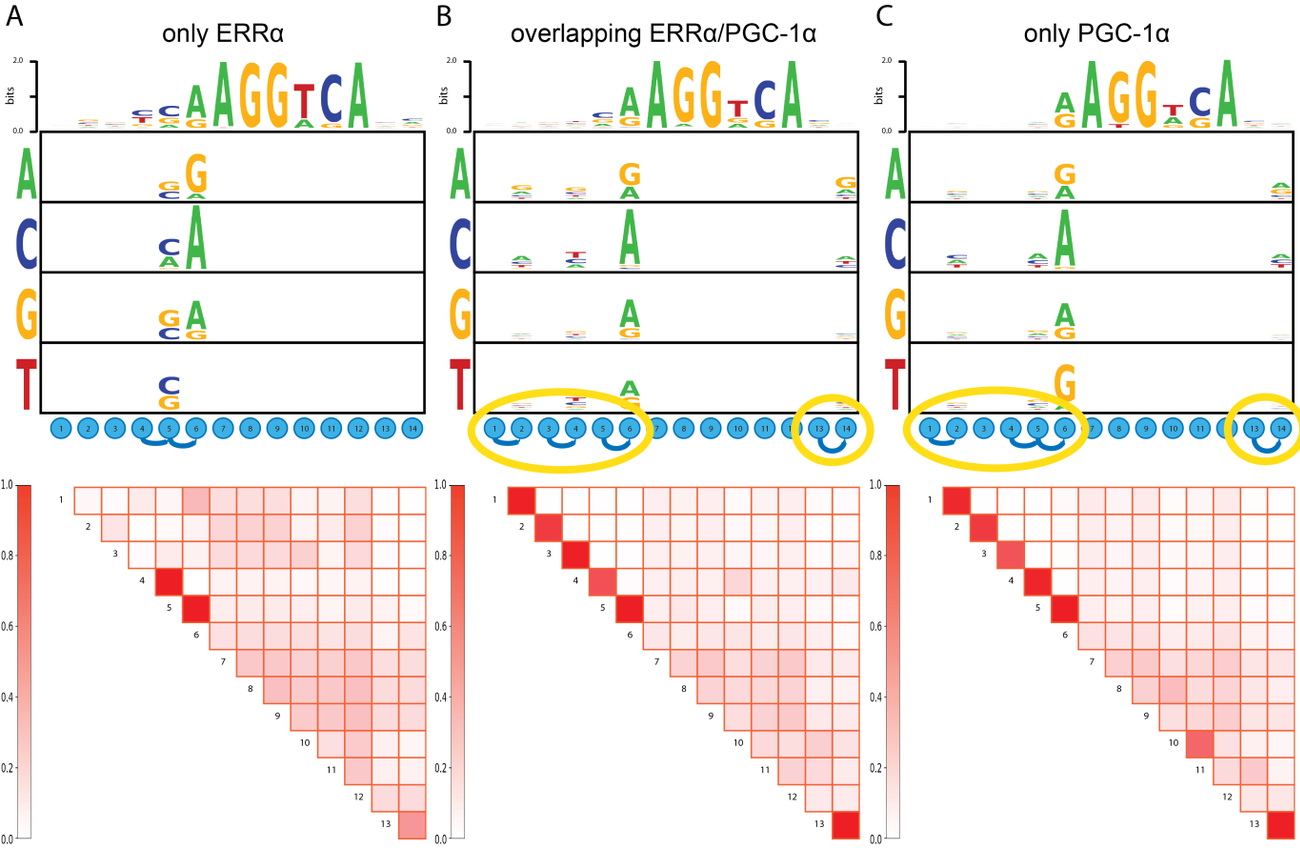

D

	only ERRα peaks	ovl. ERRα/PGC-1α peaks	only PGC-1α peaks
posterior sum dimers	599.15	1354.69	3475.18
posterior sum monomers	378.88	432.60	1456.84
ratio monomers/dimers	0.63	0.32	0.42
ratio monomers/(monomers+dimers)	0.39	0.24	0.30

Figure 3

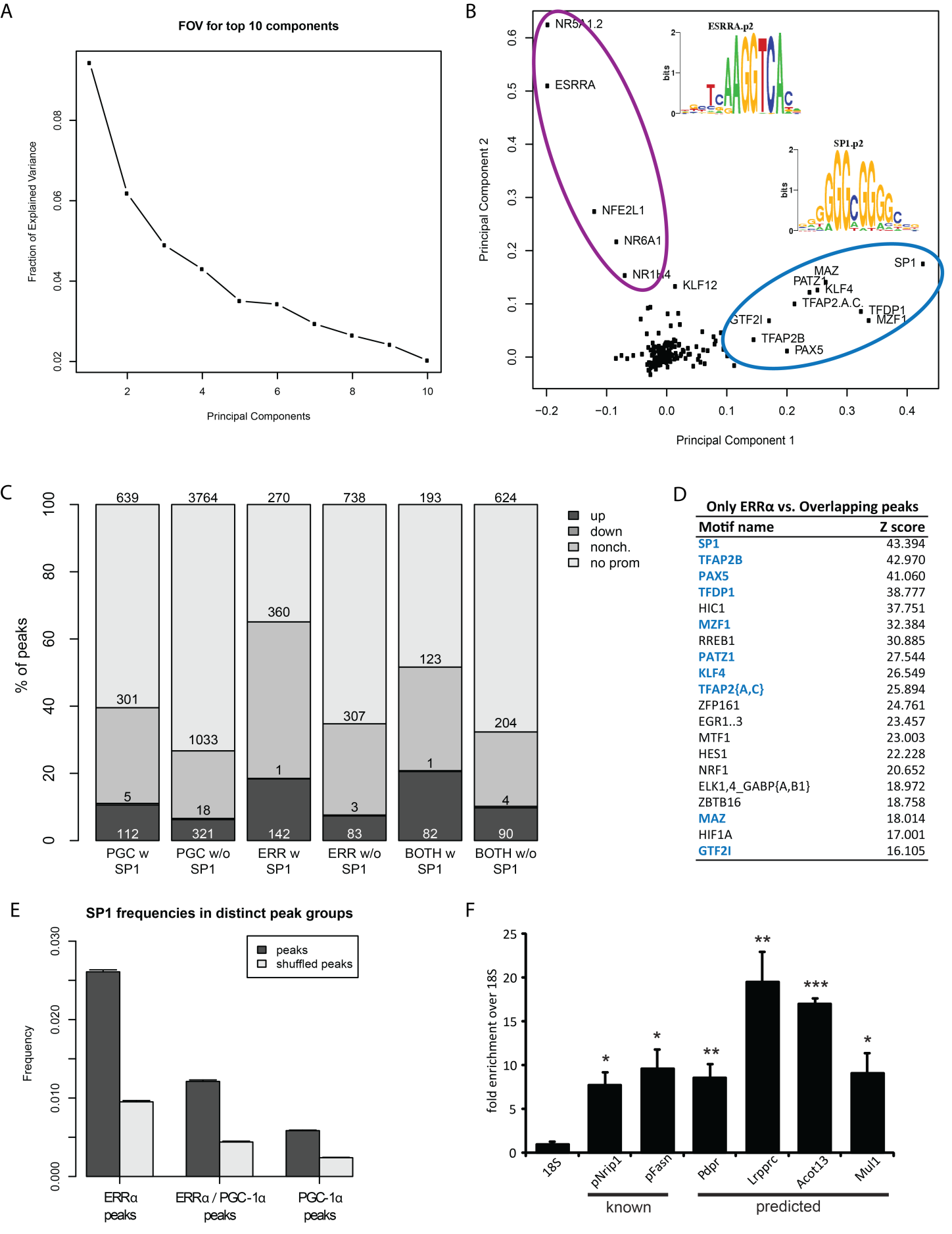

Only ERRα vs. Overlapping peaks

Motif name	Z score
SP1	43.394
TFAP2B	42.970
PAX5	41.060
TFDP1	38.777
HIC1	37.751
MZF1	32.384
RREB1	30.885
PATZ1	27.544
KLF4	26.549
TFAP2{A,C}	25.894
ZFP161	24.761
EGR1..3	23.457
MTF1	23.003
HES1	22.228
NRF1	20.652
ELK1,4_GABP{A,B1}	18.972
ZBTB16	18.758
MAZ	18.014
HIF1A	17.001
GTF2I	16.105

Figure 4

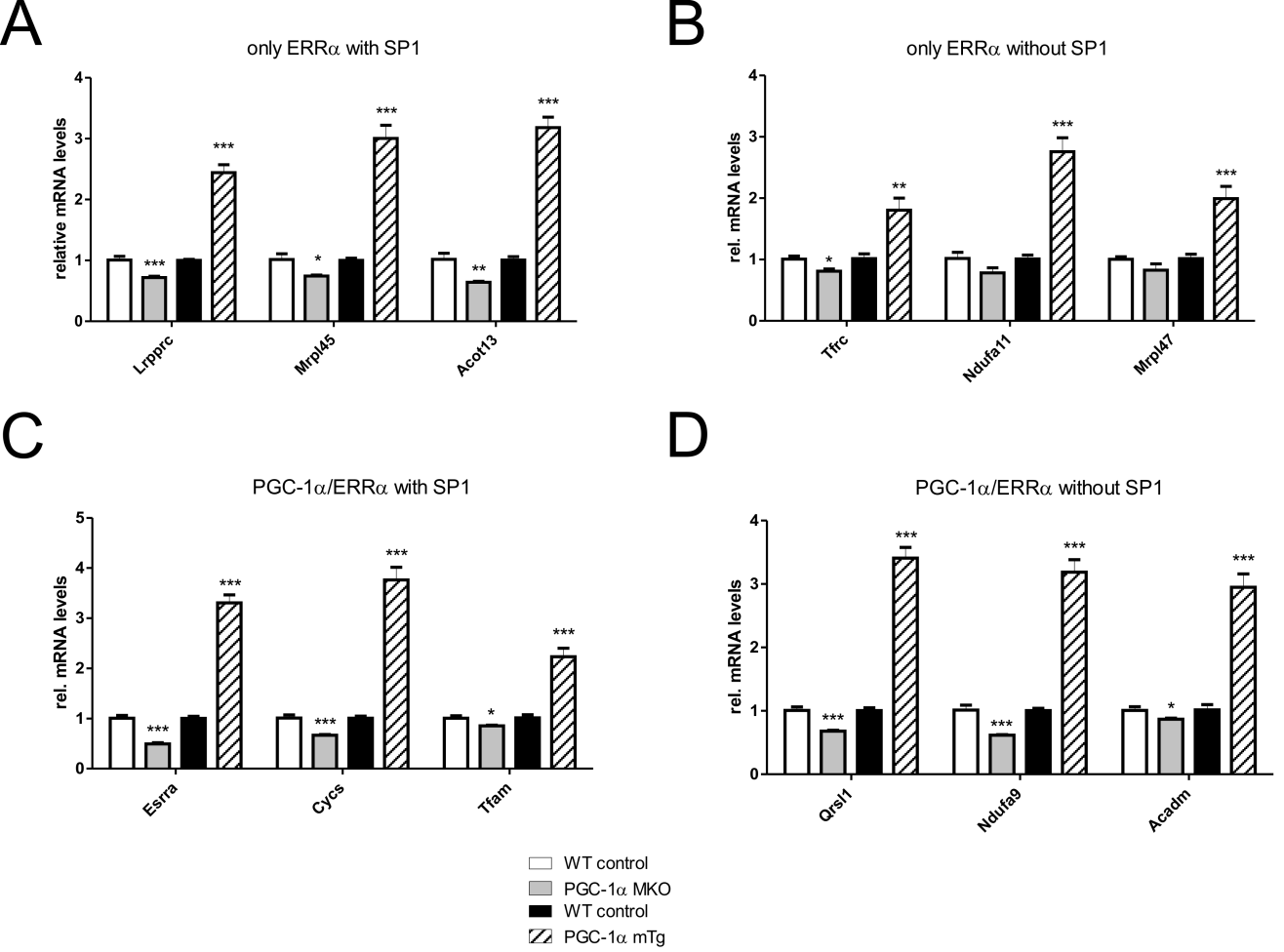
A
only ERRα with SP1
relative mRNA levels
0
1
2
3
4
***
*
**
Lrpprc
Mrpl45
Acot13
B
only ERRα without SP1
rel. mRNA levels
Tfrc
Ndufa11
Mrpl47
C
PGC-1α/ERRα with SP1
rel. mRNA levels
5
Esrra
Cycs
Tfam
D
PGC-1α/ERRα without SP1
rel. mRNA levels
Qrsl1
Ndufa9
Acadm
WT control
PGC-1α MKO
WT control
PGC-1α mTg

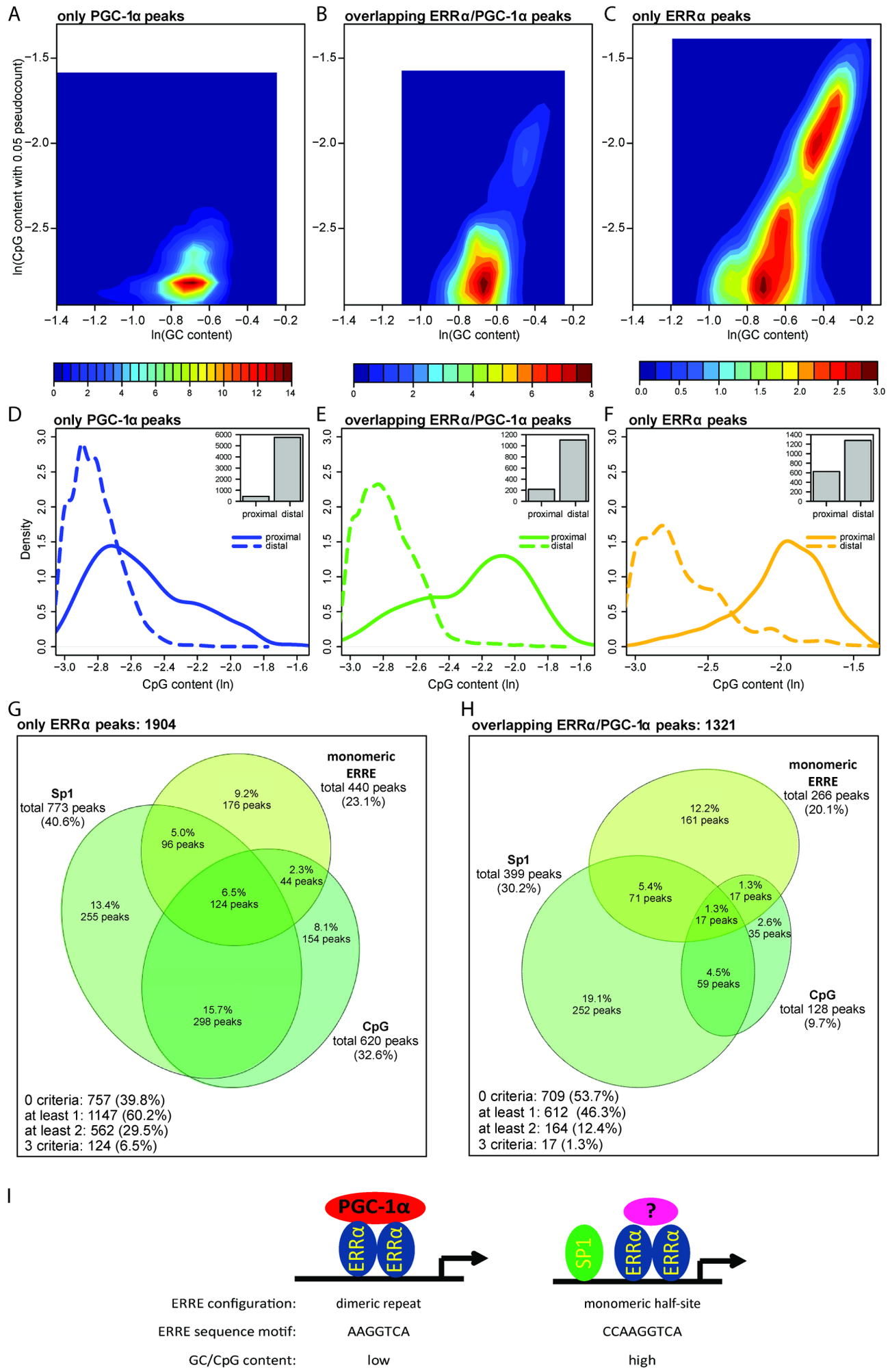
A
only PGC-1α peaks
B
overlapping ERRα/PGC-1α peaks
C
only ERRα peaks
ln(CpG content with 0.05 pseudocount)
ln(GC content)
D
E
F
Density
CpG content (ln)
proximal
distal
G
only ERRα peaks: 1904
Sp1
total 773 peaks
(40.6%)
monomeric
ERRE
total 440 peaks
(23.1%)
CpG
total 620 peaks
(32.6%)
9.2%
176 peaks
5.0%
96 peaks
2.3%
44 peaks
6.5%
124 peaks
13.4%
255 peaks
8.1%
154 peaks
15.7%
298 peaks
0 criteria: 757 (39.8%)
at least 1: 1147 (60.2%)
at least 2: 562 (29.5%)
3 criteria: 124 (6.5%)
H
overlapping ERRα/PGC-1α peaks: 1321
Sp1
total 399 peaks
(30.2%)
monomeric
ERRE
total 266 peaks
(20.1%)
CpG
total 128 peaks
(9.7%)
12.2%
161 peaks
5.4%
71 peaks
1.3%
17 peaks
1.3%
17 peaks
2.6%
35 peaks
4.5%
59 peaks
19.1%
252 peaks
0 criteria: 709 (53.7%)
at least 1: 612 (46.3%)
at least 2: 164 (12.4%)
3 criteria: 17 (1.3%)
I
PGC-1α
ERRα
ERRα
SP1
?
ERRα
ERRα
ERRE configuration:
dimeric repeat
monomeric half-site
ERRE sequence motif:
AAGGTCA
CCAAGGTCA
GC/CpG content:
low
high

Supplementary figures and tables

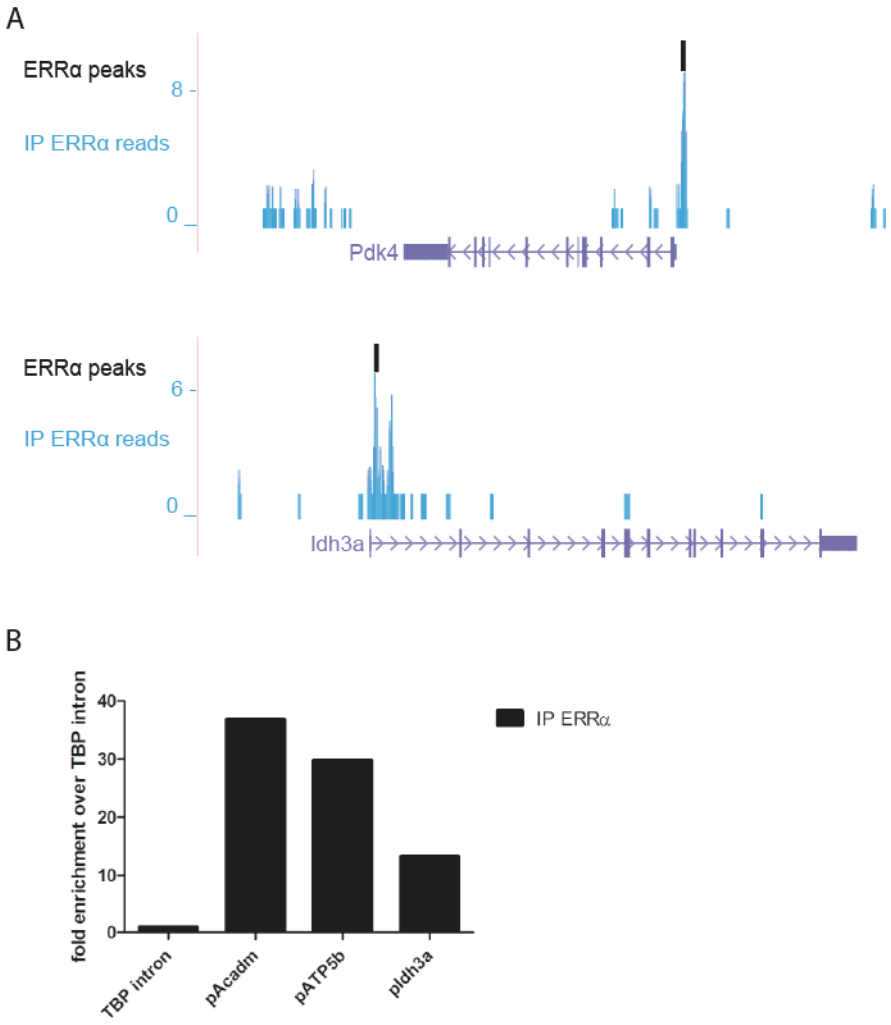

Suppl. Figure S1. (**A**) ERRα read densities around the TSS of the known target genes Pdk4 and Idh3a, as displayed by the UCSC Genome Browser. (**B**) Real-time semiquantiative PCR validation of the ChIP enrichment measured at the promoter of a set of ERRα target genes. Bars represent fold enrichment over that of the TBP intron.

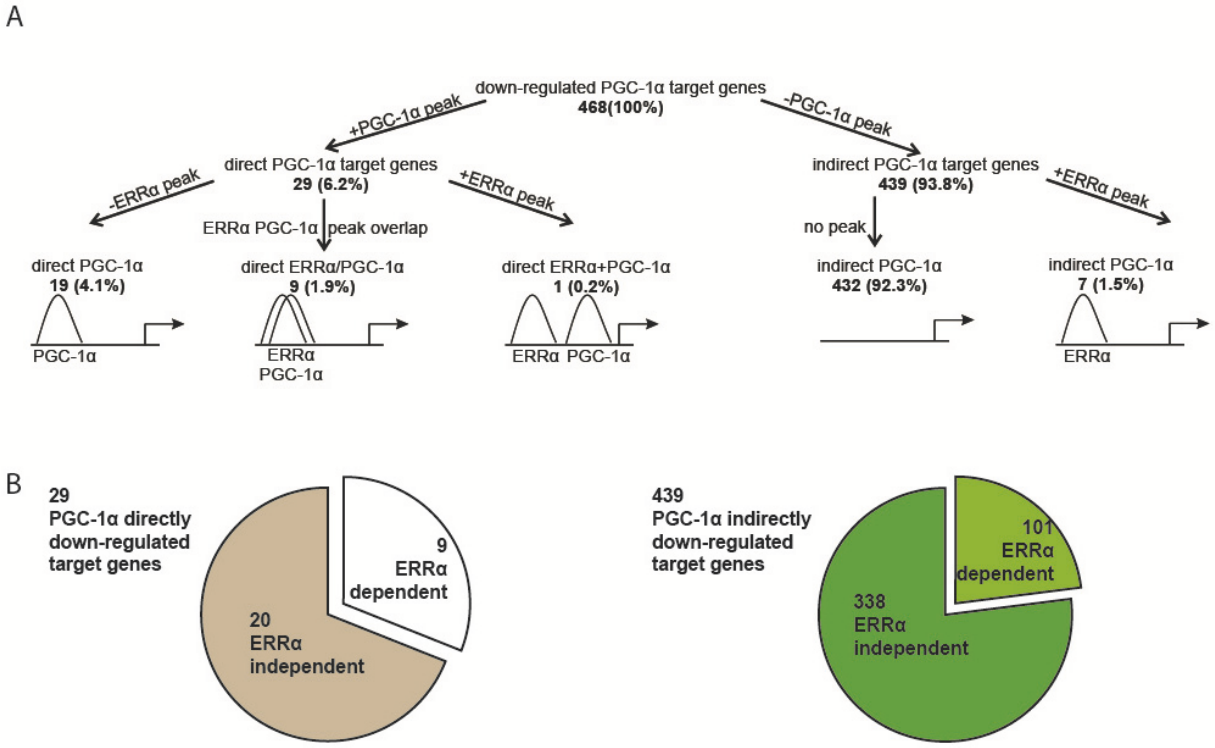

Suppl. Figure S2. (**A**) Tree diagram of all PGC-1α down-regulated target genes, distinguished in different subgroups according to peak presence/absence. (**B**) Piechart representing the classification of directly (grey/white) and indirectly (dark green/light green) down-regulated PGC-1α target genes, either ERRα-dependent or ERRα-independent targets.

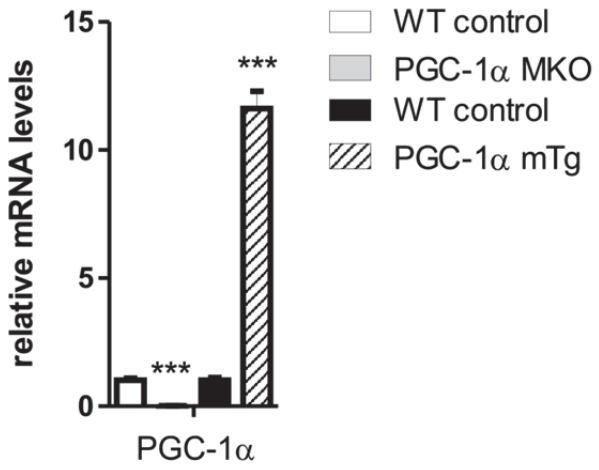

Suppl. Figure S3. Gene expression of PGC-1α in muscle-specific knockout mice (MKO), muscle-specific transgenic animals (mTg) and their respective wildtype control littermates.

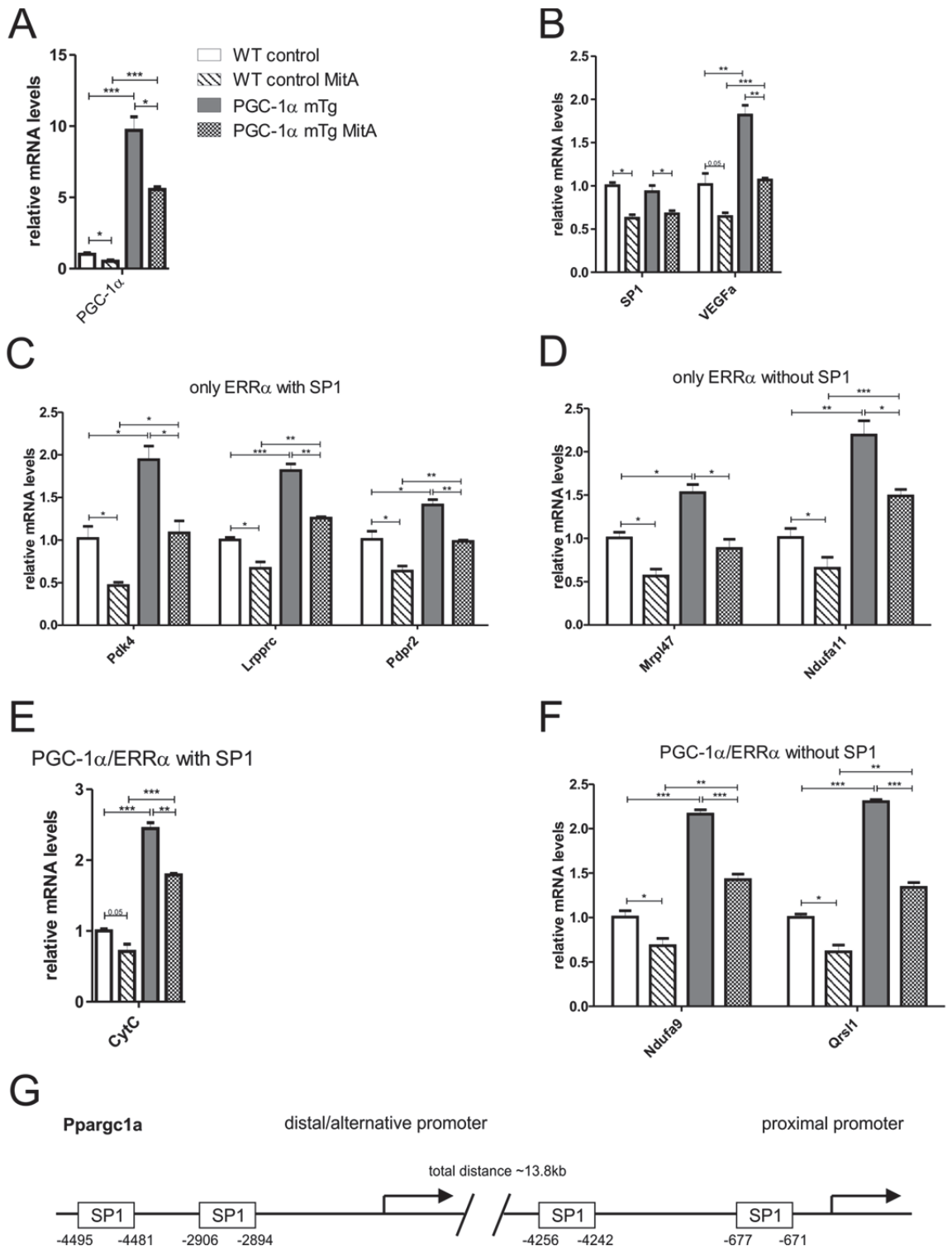

Suppl. Figure S4. Gene expression changes upon pharmacological inhibition of SP1 with Mithramycin A (MitA) in mouse muscles *in vivo*. (A) Expression of endogenous and transgenic PGC-1α in muscle-specific transgenic mice (mTg) and wildtype littermate controls with and without MitA, respectively. **(B)** Inhibition of known SP1 target genes by MitA (see Suppl. Refs. (1-3). **(C-F)** Regulation of PGC-1α-controlled gene expression by inhibition of SP1 with only ERRα peaks and SP1 binding sites **(C)**, only ERRα peaks without SP1 binding sites **(D)**, overlapping PGC-1α/ERRα peaks with SP1 binding sites **(E)** and overlapping PGC-1α/ERRα peaks without SP1 binding sites **(F)**, respectively. **(G)** Representation of predicted SP1 binding sites in the proximal and distal PGC-1α promoter regions. Predictions were made with MatInspector and PROMO (see Suppl. Refs. 4,5).

Suppl. Table 1. Real-time qPCR primer sequences

Real-time qPCR primers for ChIP validation		
Gene promoter or intron	*Forward primer*	*Reverse primer*
TBP intron	TGTGAGCTCCTTGGCTTTTT	ATAGTTGCCCAGCAATCAGG
promoter of Acadm	CCTTGCCCGAGCCTAAAC	GTCTGGCTGCGCCCTCT
promoter of ATP5b	CTGGAAACTTCCACCCTCACTA	GAGAGGTTTTTGGCGGAACTA
promoter of Idh3a	GGACGGCGTCAAGGTCAAG	GCCTAGGTGGCCTGTCTGTG
pNrip1	CACGCCATTCAGCTCTTCAG	GTGACAATGGGAGGGAGGG
pFasn	CTGGAGCACAAGGAACGC	GGACAGAGATGAGGGCGTC
Pdpr	CACACTCGTCGTCAACCAG	GTGCGCTTGTTTGGGTCTC
Lrpprc	ACAACACCCCTCCACTTTGA	CGGTGTCGCTCCTAGTTG
Acot13	TCACTCTTTAGCGCCCCAG	AAGACCGCCCTCTCTGGT
Mul1	ACTCCATATACCGGCAGAAGG	GAGCTGCCAGTGAGACCG
Real-time qPCR primers for testing the knockdown of ERRα		
Gene	*Forward primer*	*Reverse primer*
18S	AGTCCCTGCCCTTTGTACACA	CGATCCGAGGGCCTCACTA
PGC-1α	TGATGTGAATGACTTGGATACAGACA	GCTCATTGTTGTACTGGTTGGATATG
ERRα	ACTGCAGAGTGTGTGGATGG	GCCCCCTCTTCATCTAGGAC
Acadm	AACACTTACTATGCCTCGATTGCA	CCATAGCCTCCGAAAATCTGAA
Aim1l	CCTGTTGCGTCCATAAGGGT	GCTCTGAGTTCCACATCCCC
Twf2	TGCTACCTCCTCTTCCGACT	ATAGCATCTTCAGCCGCACC
Atg9b	TGGCATCACATCCAGAACCT	CATTGTAATCCACGCAGCGA
Ifrd1	GACAAGAGAAAGCAGCGGTC	GGTACTGCATCCCTGATCCA
Real-time qPCR primers used to analyze gene expression in mouse muscle *in vivo*		
Gene	*Forward primer*	*Reverse primer*
Acadm	AACACTTACTATGCCTCGATTGCA	CCATAGCCTCCGAAAATCTGAA
Acot13	TCACTCTTTAGCGCCCCAG	AAGACCGCCCTCTCTGGT
Cycs	GCAAGCATAAGACTGGACCAAA	TTGTTGGCATCTGTGTAAGAGAATC
CytC	TGCCCAGTGCCACACTGT	CTGTCTTCCGCCCGAACA
Esrra	ACTGCAGAGTGTGTGGATGG	GCCCCCTCTTCATCTAGGAC
Lrpprc	ACAACACCCCTCCACTTTGA	CGGTGTCGCTCCTAGTTG
Mrpl45	CCAGAGGGTGATGCTCGAAT	TTCGGATTGCCAGCTGTGAT
Mrpl47	CTCGGGGTAAGTGGTGAGAG	CTCAGGACTCCTCGGAAACC
Ndufa9	TTCTGTGGCTCATCCCATCG	TGTAGCCCCAAACACAGTGG
Ndufa11	TGGTGATGTAGGTCTTGCGA	GCGTCCAAGGCGTTCAATAA
Pdk4	AAAATTTCCAGGCCAACCAA	CGAAGAGCATGTGGTGAAGGT
Pdpr2	ATGAACTCTGCTGGCCTGTC	AAGCGCTGCAAATCCAACTC
PGC-1α ex2	TGATGTGAATGACTTGGATACAGACA	GCTCATTGTTGTACTGGTTGGATATG
PGC-1 ex3-5	AGCCGTGACCACTGACAACGAG	GCTGCATGGTTCTGAGTGCTAAG
PolR2a	AATCCG CATCATGAACAGTG	CAGCATGTTGGACTCAATGC
Qrsl1	GTTGGATCAGGGTGCCCTAC	GGGGTTTCTAACTGGCCCAA
SP1	GACCTCATCTCCGAGCAC	GAAGCTCGTCCGAACGTGTA
Tfam	GAGCGTGCTAAAAGCACTGG	GCTACCCATGCTGGAAAAACA
Tfrc	AGCTTTGTCCTTTTCAGCTGT	TGTGGGGAGCCGCTGTAC
VEGFα	CACGACAGAAGGAGAGCAGA	GGGCTTCATCGTTACAGCAG

Supplemental references

1. Xie L, Collins JF. Transcription factors Sp1 and Hif2alpha mediate induction of the copper-transporting ATPase (Atp7a) gene in intestinal epithelial cells during hypoxia. *J Biol Chem.* 2013;288(33):23943-23952.
2. Malek A, Nunez LE, Magistri M, Brambilla L, Jovic S, Carbone GM, Moris F, Catapano CV. Modulation of the activity of Sp transcription factors by mithramycin analogues as a new strategy for treatment of metastatic prostate cancer. *PLoS One.* 2012;7(4):e35130.
3. Rosol TJ, Capen CC. The effect of low calcium diet, mithramycin, and dichlorodimethylene bisphosphonate on humoral hypercalcemia of malignancy in nude mice transplanted with the canine adenocarcinoma tumor line (CAC-8). *J Bone Miner Res.* 1987;2(5):395-405.
4. Quandt K, Frech K, Karas H, Wingender E, Werner T. MatInd and MatInspector: new fast and versatile tools for detection of consensus matches in nucleotide sequence data. *Nucleic Acids Res.* 1995;23(23):4878-4884.
5. Messeguer X, Escudero R, Farre D, Nunez O, Martinez J, Alba MM. PROMO: detection of known transcription regulatory elements using species-tailored searches. *Bioinformatics.* 2002;18(2):333-334.